

Chemical Activation by Electron Transfer in Charge-Transfer Complexes. Formation and Reactions of Transient Ion Radical Pairs*

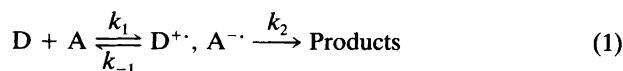
Jay K. Kochi

Department of Chemistry, University of Houston, Houston, Texas 77204-5641, USA

Kochi, J. K., 1990. Chemical Activation by Electron Transfer in Charge-Transfer Complexes. Formation and Reactions of Transient Ion Radical Pairs. – Acta Chem. Scand. 44: 409–432.

The ubiquity of charge-transfer (CT) and electron donor–acceptor or EDA complexes as precursors leading to various types of organic and organometallic reactions is underscored. Structural effects of HOMO–LUMO interactions extant in donor–acceptor pairs, as established by X-ray crystallography, are critical to the charge-transfer phenomenon in various types of weak molecular complexes. The direct relationship of the CT excited state to the activated complex is clearly delineated and emphasized in the thermal and photochemical nitration and osmylation of aromatic hydrocarbons with various nitrating agents and osmium tetroxide, respectively. The use of time-resolved picosecond spectroscopy identifies the nature of the CT ion pairs that are relevant to the transition state description of electrophile–nucleophile interactions.

Electron interchange between an inorganic oxidant and reductant is often a chemically reversible process owing to the common occurrence of thermodynamically stable redox pairs differing by a single electron. As such, electron transfer is a well-established concept in inorganic chemistry.¹ By contrast, the electron detachment from most electron-rich organic donors (D) generates transient cation radicals (from uncharged precursors), and the analogous electron attachment to electron-poor organic acceptors (A) generally affords transient anion radicals. This leads to a mechanistic situation in which the stepwise formation of products via electron transfer, i.e. eqn. (1) is kinetically difficult to



distinguish from a concerted single-step process, especially when back electron transfer (k_{-1}) and the follow-up step (k_2) are facile. Consequently, the formulations of organic and organometallic transformations involving the interactions of various types of electrophile/nucleophile, acid/base (both Brønsted and Lewis), and cation/anion pairs have usually ignored the electron-transfer pathway.

Outer-sphere and inner-sphere electron transfer

Critical to the electron-transfer formulation in eqn. (1) is the production of the ion radical pair $[D^{\cdot+}, A^{\cdot-}]$, as evaluated from the oxidation potential E_{ox}° of the donor, the

reduction potential E_{red}° of the acceptor, and ion-pairing (coulombic) energies. The dependence of the latter on the interionic separation r_{ip} is illustrated in the comparative rates of reduction of three series of acceptors A, viz., FeL_3^{3+} (L = 4- and 7-substituted 1,10-phenanthrolines), IrCl_6^{2-} and tetracyanoethylene (TCNE) by four types of sterically unique organometallic donors (RM) viz., octahedral: $(\text{CH}_3)_2\text{CoM}$ (M = tetraazamacrocycle), square-planar $(\text{CH}_3)_2\text{PtL}_2$ (L = phosphines), tetrahedral tetraalkyl-

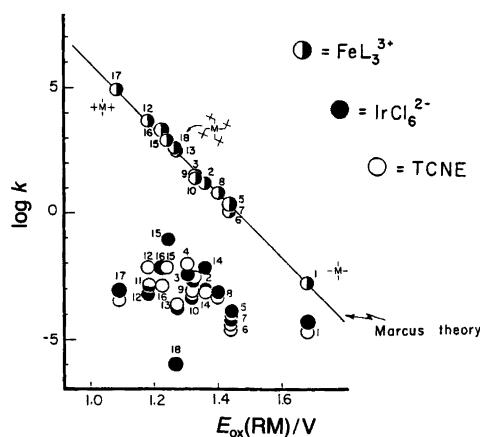
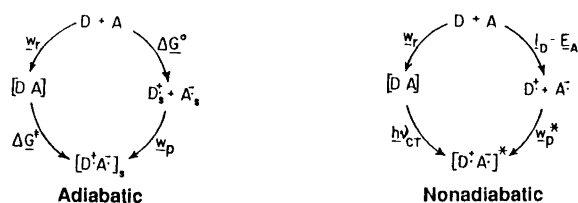


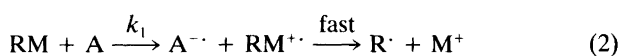
Fig. 1. Contrasting behavior of $[\text{IrCl}_6]^{2-}$ (●) and TCNE (○) relative to $[\text{Fe}(\text{phen})_3]^{3+}$ (●) in the correlation of rates of oxidation with the ionization potentials of alkylmetals R_m: 1 = Me₄Sn, 2 = Et₄Sn, 3 = nPr₄Sn, 4 = nBu₄Sn, 5 = EtSnMe₃, 6 = nPrSnMe₃, 7 = nBuSnMe₃, 8 = Et₂SnMe₂, 9 = nPr₂SnMe₂, 10 = nBu₂SnMe₂, 11 = iPr₄Sn, 12 = sBu₄Sn, 13 = iBu₄Sn, 14 = iPrSnMe₃, 15 = tBuSnMe₃, 16 = iPr₂SnMe₂, 17 = tBu₂SnMe₂, 18 = (tBuCH₂)₄Sn (Ref. 2). The slope of the $[\text{Fe}(\text{Phen})_3]^{3+}$ correlation is $-1/2$.

* Presented as part of a plenary lecture at the 32nd IUPAC Congress in Stockholm, Sweden, August 2–7, 1989.



Scheme 1.

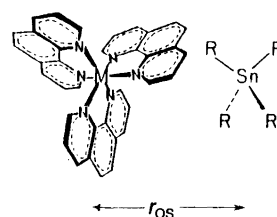
metals R_m ($m = \text{tin and lead}$), and linear dialkylmercurials that differ widely in the intermolecular separations between donor-acceptor pairs.² Since the rapid fragmentation of organometallic cation radicals renders the rate process (k_1) irreversible [eqn. (2)] the plots of the measured



rates in Fig. 1 represent the free energy correlations for electron transfer.

The fit of the kinetic data for $A = \text{Fe}(\text{Phen})_3^{3+}$ to the Marcus theory for outer-sphere electron transfer is unmistakable. Importantly, the inclusion of the highly ligand-encumbered tetra-n-propyltin (No. 18) in the same Marcus correlation as tetramethyltin (No. 1) indicates that steric effects are unimportant in the transition state for the redox pair $\text{Fe}(\text{Phen})_3^{3+}/RM$ – as expected for outer-sphere electron transfer. By the same reasoning, the marked deviations of all the kinetic data for $A = \text{IrCl}_6^{2-}$ and TCNE point to a distinctively different transition state for electron transfer with these sterically more accessible acceptors. Furthermore, the marked negative deviation of the oxidation of tetra-n-propyltin by IrCl_6^{2-} and TCNE (k_1 too slow to measure) is diagnostic of a severely congested transition state with a sizeable inner-sphere component. The latter is quantitatively evaluated by the inner-sphere work term w_p for the ion pair formation as presented in the thermochemical cycle for adiabatic electron transfer above (Scheme 1).³ Indeed the linear free energy correlation in Fig. 2 shows that the inner-sphere work term can be experi-

mentally evaluated from the non-adiabatic counterpart w_p^* as it is obtained from the charge-transfer or CT spectra of the corresponding series of inner-sphere complexes [TCNE, RM] of the type to be described later. Consequently we propose that the strong modulating effect of steric congestion in the organometal donors on the rates of electron transfer to IrCl_6^{2-} serves as an experimental criterion to distinguish inner-sphere from outer-sphere processes. As applied to the ion-pair formulation in Scheme 1, the outer-sphere electron transfer generates an ion pair



with a mean interionic separation r_{OS} sufficient to leave the coordination sphere of the organometal donor largely unperturbed, as pictorially represented above (ionic charges not indicated).

Steric compression of ligands is diagnostic of a more constrained inner-sphere pathway for electron transfer with a diminished mean ion-pair separation r_{IS} . The strong similarity of the free energy correlation in Fig. 2 indicates that r_{IS} for IrCl_6^{2-} is akin to the mean separation r_{CT} in the TCNE oxidation – both related to the change in the tetrahedral organometal to a trigonal bipyramidal configuration, i.e.

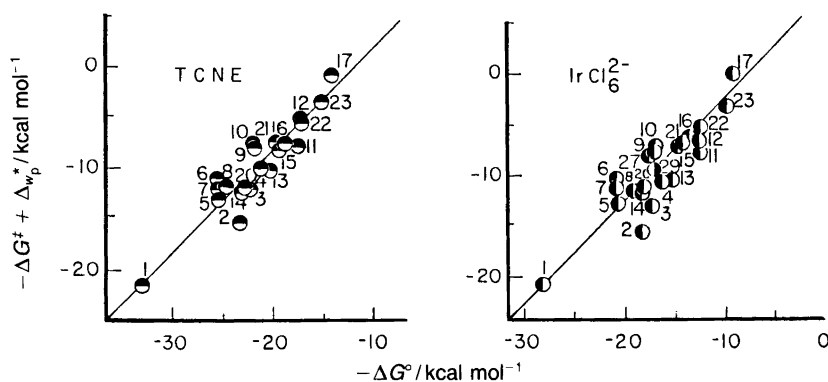
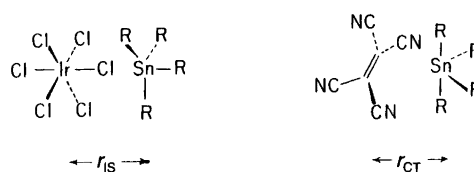
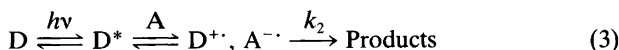


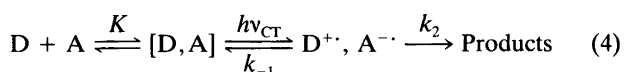
Fig. 2. Free energy relationship for electron transfer based on the thermochemical cycles in Scheme 1 for the oxidation of organometals (as listed in Fig. 1) with (left) tetracyanoethylene and (right) hexachloroiridate(IV).

Photochemical activation of electron transfer

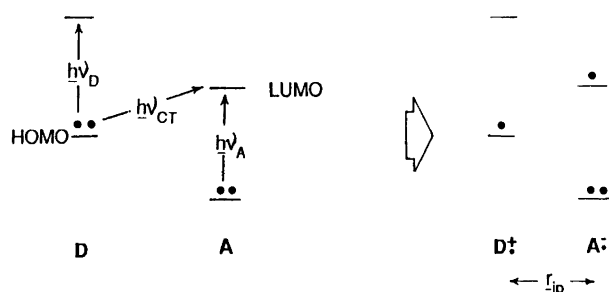
Photochemical electron transfer proceeds either by the prior actinic activation of the organic donor followed by quenching by the electron acceptor [eqn. (3)], or the re-



verse sequence involving the prior activation of the acceptor and quenching with the donor.⁴ Photochemical electron transfer can also be effected by the irradiation of the charge-transfer (CT) absorption band of the precursor (EDA) complex,⁵ [eqn. (4)]. The irradiation of the charge-



transfer band of the EDA complex in eqn. (4) is the more direct method for the photoactivation of electron-transfer oxidation, since the absorbed energy $h\nu_{CT}$ is directly applied to the conversion of a bonding electron in the HOMO of the donor D into an antibonding electron in the LUMO of the acceptor A. Such a spontaneous generation of $[D^{+\cdot}, A^{-\cdot}]$ represents the contact (inner-sphere) ion pair (CIP)⁶ in Scheme 2 with an interionic separation r_{ip} that is essentially that originally present in the EDA precursor $[D, A]$.⁷ However in the alternative mode of photoactivation [eqn. (3)], the excitation of only D (see $h\nu_D$ in Scheme 2) is



Scheme 2.

followed by electron transfer to A in a subsequent step. Since the latter takes place by a diffusional process,⁴ $[D^{+\cdot}, A^{-\cdot}]$ is not necessarily the same contact (inner-sphere) ion pair formed by the direct charge-transfer activation. Indeed, there are examples of diffusional quenching by electron transfer over long distances to form initially a less intimate, solvent-separated (outer-sphere) ion pair (SSIP).⁸ The same situation pertains to the photoinduced electron-transfer oxidation by the prior excitation of the acceptor (see $h\nu_A$ in Scheme 2). The modulating effect of varying ion-pair structures lies at the core of electron-transfer oxidation, as will be elaborated in the following sections.

Charge-transfer activation. Although the direct CT process for photoinduced electron transfer does not depend on

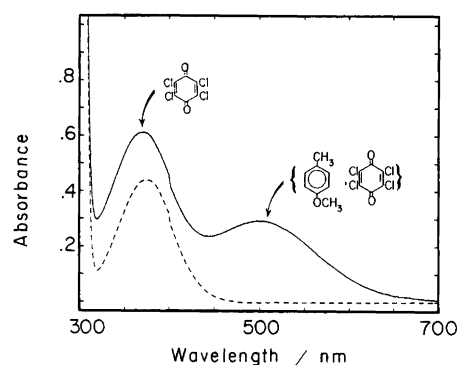
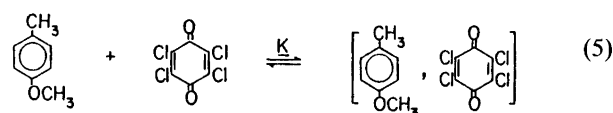
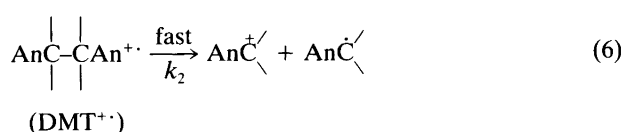


Fig. 3. Absorption spectra of 2.0×10^{-3} M chloranil alone (-----) and with 0.4 M *p*-methoxytoluene (—) in dichloromethane.

diffusional quenching that complicates the kinetics analysis of the more conventional sensitization methods, its exploitation is often frustrated by an efficient electron transfer (k_{-1}).⁹ This limitation can be addressed with labile acceptor moieties ($A^{-\cdot}$) like that from tetranitromethane¹⁰ and donor cations ($D^{+\cdot}$) derived from strained hydrocarbons,¹¹ which undergo unimolecular decomposition with rate constants comparable to k_{-1} . Indeed the latter underscores the need for a related series of highly labile donor cations to enhance the efficiency of charge-transfer photochemistry. Thus the use of arene donors derived from *p*-methoxytoluene (MT) in which the presence of the common chromophore allows the direct comparison of charge-transfer and sensitized photochemistry as described by Jones and coworkers.¹² For example, the absorption spectrum in Fig. 3 shows the simultaneous appearance of two resolved bands – one arising from the local excitation of the chloranil acceptor (CA) and the other from the CT excitation of the 1:1 EDA complex [eqn. (5)]. The spectrophotometric



determination of the formation constant in eqn. (5) according to the Benesi-Hildebrand procedure¹³ indicates $K = 0.3$ M⁻¹ in dichloromethane. In such weak EDA complexes, photophysical and photochemical studies by time-resolved spectroscopy (*vide infra*), as well as Mulliken theory¹⁴ point to $[\text{MT}^{+\cdot}, \text{CA}^{-\cdot}]$ as the pertinent ion radical pair in eqn. (4). In order to promote the CT photochemistry in eqn. (4), the methoxytoluene chromophore is utilized in various dimeric structures DMT that are known to yield highly unstable cation radicals¹⁵ [eqn. (6)], where $\text{An} = p$ -



MeOC_6H_4 . It is important to emphasize that the donor property of every DMT listed in Table 1 is essentially the

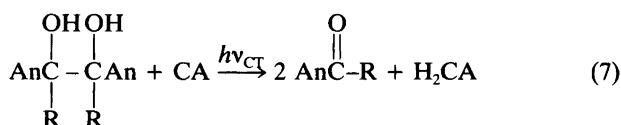
Table 1. Charge-transfer and sensitized photochemistry or methoxytoluene donors with chloranil.^a

DMT Donor ^b	$h\nu_{CT}/eV^c$	Φ_{CT}^d	Φ_{sens}^e	$\tau/10^{10} s^{-1}$	Products ^f
[An ₂ COT] ₂	–	0.18	0.87	1.1	An ₂ CO, T ₂ CA
[An ₂ COH] ₂	2.58	0.22	0.94	0.86	An ₂ CO, H ₂ CA
[AnCMeOT] ₂	2.56	0.12	0.75	1.8	AnCOMe, T ₂ CA
[AnCMeOH] ₂	–	0.15	0.69	1.4	AnCOMe, H ₂ CA
[AnCHOH] ₂	2.58	0.03	0.84	7.9	AnCHO, H ₂ CA
[AnCHOT] ₂	2.56	0.01	0.81	24	AnCHO, T ₂ CA
[AnCMe ₂] ₂	2.51	<0.001	0.25	>200	AnC(Me)=CH ₂ , H ₂ CA
[AnCH ₂] ₂	2.49	0	0.01	–	(AnCH) ₂ , H ₂ CA

^aIn dichloromethane containing 0.04 M anisyl donor and 0.02 M chloranil. ^bT = (CH₃)₃Si. ^cMT, 2.46 eV. ^dAt λ 505 \pm 5 nm. ^eAt λ 405 \pm 5 nm. ^fHigh yields (>90 %) based on stoichiometry in eqn. (7).

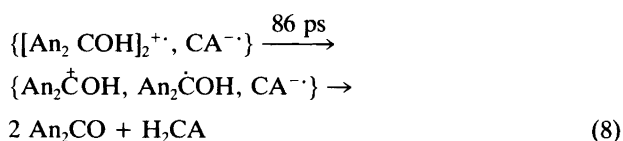
same as that of the parent (MT), as quantitatively judged by the invariant positions of the CT bands (see column 2).

Electron-transfer photochemistry resulting from the selective irradiation of only the charge-transfer band is strongly dependent on the side-chain substitution pattern on the DMT donor. Thus the pinacols are quantitatively cleaved in the presence of one equivalent of chloranil according to the stoichiometry of eqn. (7), where R = An,



Me and H. Moreover the bis(trimethylsilyl) ethers of the pinacols are similarly cleaved to 2 mol equiv. of dimethoxyphenyl ketone, methoxyphenyl methyl ketone or anisaldehyde and one mol equiv. of the bis(trimethylsilyl) ether of tetrachlorohydroquinone, as listed in Table 1. In strong contrast, the bibenzyl derivatives [AnCH₂]₂ and [AnC(Me)₂]₂ remain singularly unchanged, even upon prolonged irradiation of the CT absorption band.

The quantum yields $\Phi_{CT} = k_2/(k_2 + k_{-1})$ for charge-transfer photochemistry as listed in column 3 lead to the lifetimes (τ) of the cation radicals in column 5 when the measured rate constant $k_{-1} = 4.1 \times 10^{10} s^{-1}$ is used to evaluate the back electron transfer. Thus the lifetime of 86 ps for [An₂COH]₂⁺ is sufficient to ensure its unimolecular fragmentation within the inner-sphere ion pair [see eqn. (4)], followed by intracage proton transfer to yield the products in eqn. (7), i.e., [eqn. (8)].



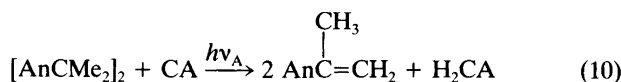
The lifetime of [AnCHOH]₂⁺ which is an order of magnitude longer than that of [An₂COH]₂⁺ accords with the

expected difference in driving force for secondary/tertiary benzylic scissions. Furthermore the absence of CT photochemistry from the bibenzyl analogues indicates that the fragmentation rates of their cation radicals are too slow to compete effectively with back electron transfer in the inner-sphere ion pair.

Activation by sensitization (diffusional quenching). The clean spectral separation of the chloranil absorption (λ_{max} 375 nm) from the CT absorption in Fig. 3 also allows the separate evaluation of the efficacy of pinacolic cleavage via the diffusional quenching of the locally excited acceptor [eqn. (9)].¹⁶



The latter ($h\nu_A$) is achieved with a narrow bandpass interference filter (λ 405 \pm 5 nm) for the specific excitation of only chloranil. The results in column 4 show consistently high efficiencies (Φ_{sens}) for the sensitized photochemistry of the pinacols and their silyl derivatives. Importantly, complete product analyses established the stoichiometry to be *identical* with that obtained by CT photochemistry. Moreover the bibenzyl analogues [AnCMe₂]₂ and [AnCH₂]₂ undergo photofragmentation and elimination according to the following stoichiometries given in eqns. (10) and (11). In

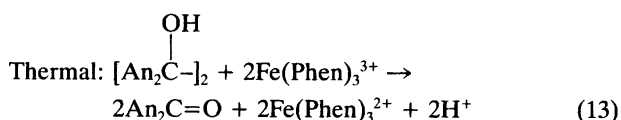
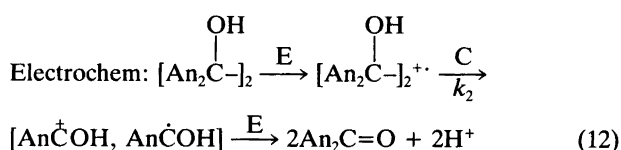


both cases, the products of the sensitized photochemistry accord with prior electron transfer followed by the known fragmentation [eqn. (10)] or proton transfer [eqn. (11)] of the cation radical (DMT⁺).¹⁷

The significantly enhanced values of Φ_{sens} for sensitized photofragmentation compared with Φ_{CT} for CT activation are undoubtedly related to the longer lifetimes of the donor cation radical (DMT⁺) in the outer-sphere ion pair. Part of

the difference in their lifetimes can be attributed to the change in spin multiplicity required for back electron transfer from the triplet ion radical pair $^3[\text{DMT}^{\cdot+}, \text{CA}^{\cdot-}]$. However, there are other complicating factors introduced by diffusional quenching, especially the ambiguity in the distance dependence of electron transfer¹⁸ to generate solvent-separated (outer-sphere) and contact (inner-sphere) ion pairs.⁸ As such, we believe that the series of labile $\text{DMT}^{\cdot+}$ with variable lifetimes evaluated by the CT process will prove to be invaluable aids as chemical clocks¹⁹ to unravel the complex photochemical kinetics stemming from different types of ion pairs relevant to outer-sphere and inner-sphere electron transfer.

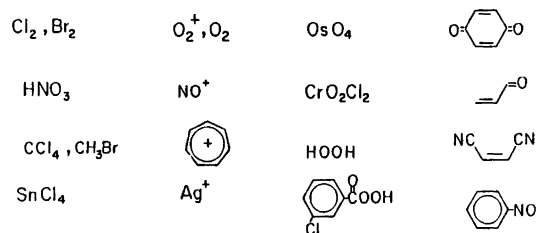
Comparative efficiencies of photochemical and thermal electron transfer. The non-adiabatic processes leading to the photo-induced electron transfer, as just described for the retro-pinacol transformation, have their counterparts in adiabatic electron transfers effected electrochemically and chemically. Thus the anodic oxidation of benzpinacol occurs by an initial one-electron transfer.^{20a} The formation of the pinacol cation-radical is followed by a rapid (k_2) carbon-carbon bond scission and further oxidation as outlined in the ECE process of eqn. (12).



The outer-sphere oxidant $\text{Fe}(\text{Phen})_3^{3+}$ effects the same retro-pinacol reaction [eqn. (13)], in which the second-order kinetics follow from the rate-limiting electron transfer to generate the same benzpinacol cation radical.^{20b} Generally, the thermal electron-transfer oxidation of a particular organic donor D, in eqn. (1) requires a stronger oxidant (i.e., A with more positive E_{red}°) than its photochemical counterparts in eqns. (3) and (4) owing to the contribution from the input of light energy (Scheme 2). Under these conditions, the driving force for back electron transfer is diminished and leads to longer lifetimes of the cation radical $\text{D}^{\cdot+}$. As a result, unimolecular processes such as the ion-radical fragmentation in eqn. (6) can more effectively compete with back electron transfer. To illustrate this point, the carbon-carbon bond cleavage of bicumyl by electron transfer to cerium(IV) occurs in high yields.^{15c} By contrast, the photoinduced cleavage of bibenzyls by quenching the chloranil triplet is inefficient ($\Phi_{\text{sens}} \sim 10^{-2}$) and the charge-transfer process non-existent (see Table 1, column 3, entries 7 and 8).

Electron donor-acceptor (EDA) complexes as intermediates

The formation of the ion radical pair $[\text{D}^{\cdot+}, \text{A}^{\cdot-}]$ is the most unequivocal indication of the viability of electron-transfer processes. However, the independent proof of the ion radical pair is generally lacking in adiabatic processes owing to its expectedly transient existence. Thus the ion-radical pair cannot be observed as a reactive intermediate since its rate of annihilation will perform always be faster than its rate of production. Charge-transfer activation in eqn. (4) presents an alternative approach to this problem since it leads to the spontaneous transformation of the donor-acceptor complex $[\text{D}, \text{A}]$ to the ion-radical pair $[\text{D}^{\cdot+}, \text{A}^{\cdot-}]$. Indeed the EDA complex shares common features with the precursor or encounter complex in this formulation of adiabatic electron transfer. Most importantly, their ubiquitous occurrence pervades the spectrum of electron donor-acceptor interactions. For example, merely consider the exposure of simple aromatic donors to the diverse classes of reagents below that include various types of electrophiles, cations, oxidants, carbonyl, and nitro compounds, etc.



In each case there is evidence for the formation of EDA complexes of the electron-poor reagent (A) with the arene donor. Both η^2 and η^6 arene complexes have been isolated and structurally characterized by X-ray crystallography. Included in Fig. 4 are the bromine-benzene, carbon tetrabromide-xylene, tetracyanobenzene-hexamethylbenzene and related weak complexes with formation constants typically $K < 1 \text{ M}^{-1}$. Nonetheless the correlations in Fig. 5 typify the direct correspondence of the charge-transfer absorption ($h\nu_{\text{CT}}$) with various types of acceptors, independent of whether they involve η^2 or η^6 bonding to the arene donor.

Direct observation of transient ion pairs by charge-transfer activation of EDA complexes

According to eqn. (4) the formation of the ion radical pair occurs upon excitation of the charge-transfer band of the EDA complex. The experimental proof of Mulliken theory¹⁴ is established in the donor-acceptor complex of 9-cyanoanthracene (CNA) and tetracyanoethylene (TCNE) shown in Fig. 6(a).⁷ Thus the deliberate excitation of the charge-transfer band at $\lambda_{\text{max}} 630 \text{ nm}$ with a 25 ps laser pulse leads to the series of time-resolved spectra in Fig. 6(c) taken shortly after the application of the 532 nm radiation

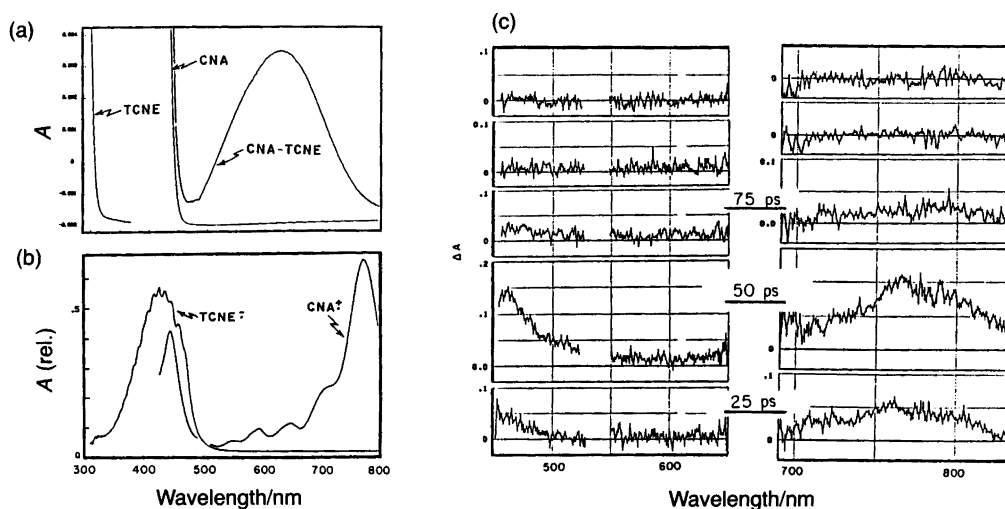
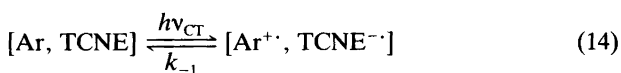


Fig. 6. Electronic absorption spectra of (a) the EDA complex of 9-cyanoanthracene (CNA) and tetracyanoethylene (TCNE) in comparison with the uncomplexed CNA and TCNE; (b) the donor cation $\text{CNA}^{+\cdot}$ and acceptor anion $\text{TCNE}^{-\cdot}$ generated spectroelectrochemically and (c) time-resolved ps absorption spectra taken at 25, 50, 75 and 100 ps following the CT excitation at 532 nm of $[\text{CNA}, \text{TCNE}]$ with a 25 ps laser pulse.

from a Nd^{3+} : YAG laser. The transient absorption bands at λ 770 and 440 nm immediately following the 25 ps laser pulse clearly delineate the simultaneous appearance of the 9-cyanoanthracene cation radical ($\text{CNA}^{+\cdot}$) and the tetracyanoethylene anion radical ($\text{TCNE}^{-\cdot}$) as shown by comparison with the absorption spectra in Fig. 6(b) of these ion radicals generated spectroelectrochemically at a platinum-mesh anode and cathode, respectively.

There is no evidence from the picosecond absorption data for either the existence of an excited state of the EDA complex or the formation of any intermediate states or species other than $\text{CNA}^{+\cdot}$ and $\text{TCNE}^{-\cdot}$. Electron transfer from the aromatic donor to TCNE thus effectively occurs in the EDA complex with the absorption of the ($h\nu_{\text{CT}}$) photon [eqn. (14)]. The transient existence of the ion pair with a

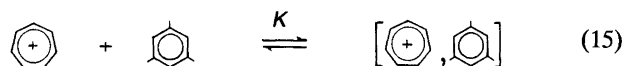


lifetime of ca. 50 ps corresponds to the electronic relaxation of the ion pair by back electron transfer ($k_{-1} \approx 2 \times 10^{10} \text{ s}^{-1}$). Such an experimental observation therefore represents the direct confirmation of the Mulliken theory, in which the irradiation of the charge-transfer band of an EDA complex consisting of a relatively non-polar ground state leads to the production of the ion radical pair $[\text{D}^{+\cdot}, \text{A}^{-\cdot}]$. Since this photo-induced electron transfer derives from an EDA complex $[\text{D}, \text{A}]$ by a vertical transition, the interionic separation r_{ip} in the CT ion pair is considered to be akin to the contact or inner-sphere ion pair described earlier.

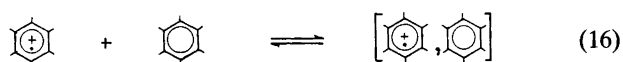
In order to establish the generality of ion radical pair formation by charge-transfer activation of EDA complexes, we now focus on a few selected examples of diverse types of acceptors interacting with arene donors.

Carbocations as electron acceptors in aromatic EDA complexes

Organic cations are electron acceptors by virtue of their electron-deficient centers on one or more carbon atoms. Indeed the coordinative unsaturation in such stable carbocations as tropylium (C_7H_7^+) and triphenylcarbenium (Ph_3C^+) is underscored by their well-known ability to form acid-base complexes with even such weak σ -donors as ethers, nitriles, etc. In a similar vein are the intermolecular interactions of tropylium ions with electron-rich anionic donors to form charge-transfer salts that are manifested by the appearance of new absorption bands in the UV/vis region, both in solution and in the crystalline salt.²¹ Less obvious are the charge-transfer absorption bands that have been observed between the tropylium or the triphenylcarbenium cation and a series of aromatic π -donors.²² The electron donor-acceptor or EDA interactions in such arene complexes are weak, as shown by the limited magnitude of the formation constant of the 1:1 complex [eqn. (15)] with



$K \approx 1 \text{ M}^{-1}$ in acetonitrile. These cationic EDA complexes are formally related to the arene dimer cations $(\text{ArH})_2^+$ that are generated from arenes and their cation radicals, [eqn. (16)].^{23,24}



Charge-transfer spectra of the tropylium cationic acceptor with various arene donors. A colorless solution of tropylium tetrafluoroborate or hexafluoroantimonate in aceto-

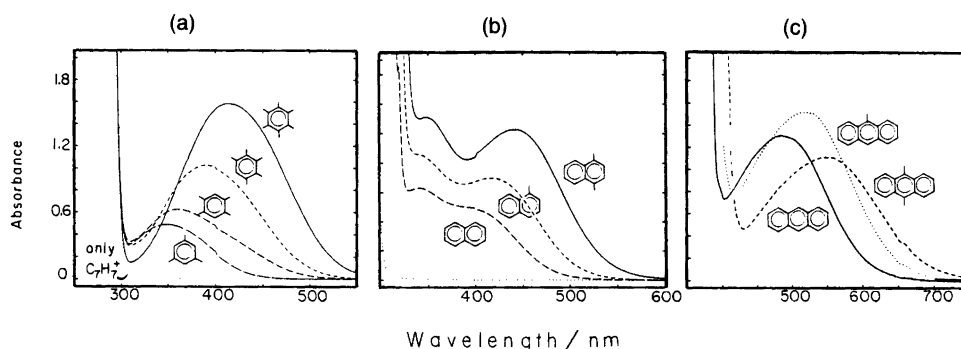
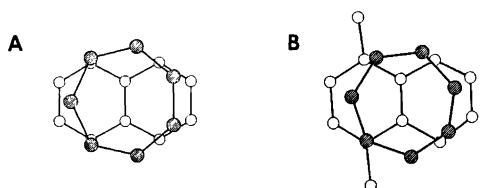


Fig. 7. Charge-transfer absorption bands of the EDA complexes of tropylium cation with various (a) benzene, (b) naphthalene and (c) anthracene donors.

nitrile turns pale yellow instantaneously upon exposure to benzene.²⁵ With naphthalene a bright lemon-yellow coloration develops; a clear red solution results from anthracene. The quantitative effects of such dramatic color changes are illustrated in Fig. 7 by the appearance of distinctive charge-transfer bands. For the series of methylbenzene donors, the absorption maxima λ_{CT} are progressively red-shifted with increasing numbers of methyl substituents [Fig. 7(a)] to reflect the accompanying decrease in the ionization potentials E_i . A similar bathochromic shift of the charge-transfer band is observed in the tropylium complexes with the series of methylnaphthalenes and methylantracenes shown in Figs. 7(b) and 7(c), respectively. Such a progressive red-shift of the new absorption bands with the ionization potentials of the aromatic donors accords with Mulliken charge-transfer theory.¹⁴ Indeed for weak EDA complexes, the energy of the charge-transfer transition (i.e. $h\nu_{CT}$) relates directly to the ionization potential by the relationship: $h\nu_{CT} = E_i - E_A - w_p^*$, since the electron affinity E_A of the tropylium acceptor is a common value, and the electrostatic work term w_p^* is considered to be constant for related donors. The common CT behavior of the methylbenzenes, naphthalenes and anthracenes is underscored by the striking linear correlation expressed as: $h\nu_{CT} = 1.0 E_i - 4.8$ to encompass the energy span of almost 2 eV.

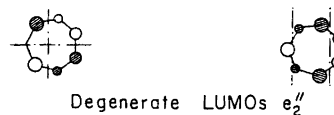
Molecular structure of tropylium EDA complexes. Despite the limited magnitudes of the formation constant ($K \sim 1 M^{-1}$) of the tropylium–naphthalene complexes in solution, crystalline complexes can be isolated. Thus the X-ray diffraction pattern from the naphthalene complex with $C_7H_7^+SbF_6^-$ obtained as bright yellow orthorhombic crystals is solved as the 1:1 EDA complex in which the planar tropylium cation is poised centrosymmetrically over the naphthalene nucleus with an interannular separation of 3.36 Å as illustrated below (A).



The related unsymmetrical donor 1,4-dimethylnaphthalene with the same tropylium salt $C_7H_7^+ SbF_6^-$ affords orange monoclinic crystals of which the X-ray crystallographic determination established the same basic centrosymmetric structure for the donor–acceptor pair, as shown above (B). Moreover, the interplanar distance from the tropylium centroid to the naphthalene plane is 3.38 Å despite the presence of two sizeable methyl substituents to lower the symmetry of the donor. Otherwise the bond distances and bond angles in the crystalline EDA complexes are essentially the same as those established earlier for the separate, uncomplexed naphthalene donors and the tropylium salt. The pair of absorption bands illustrated in Fig. 7(b) can be accounted for by the charge-transfer transitions from the highest occupied molecular orbital (HOMO) and the subjacent HOMO-1 depicted below. As such, the



centrosymmetric structures above accord with the optimum overlap of the naphthalene HOMO and HOMO-1 of a_u and b_u symmetry, respectively, with the degenerate pair of tropylium e_2'' LUMOs of the same gross symmetry. On the basis of similar considerations of orbital symmetry, neither of the EDA complexes of tropylium with benzene or with anthracene donors would be centrosymmetric.



Observation of the charge-transfer excited state by time-resolved picosecond spectroscopy of tropylium EDA complexes. In order to ascertain the nature of the colored (visible) absorption bands of the tropylium EDA complexes in Fig. 7, the time-resolved spectra can be examined immediately following the application of a 30 ps pulse consisting of the second harmonic at 532 nm of a mode-locked Nd^{3+} : YAG laser. This wavelength coincides with

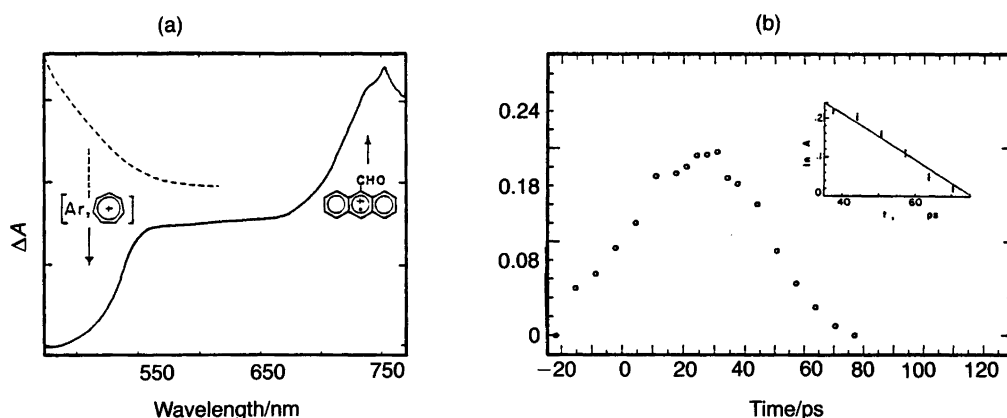
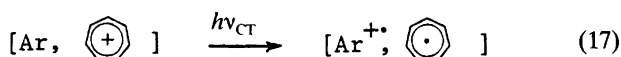


Fig. 8. (a) Typical time-resolved ps absorption spectrum following the charge-transfer excitation of tropylium EDA complexes with arenes (anthracene-9-carbaldehyde) showing the bleaching (negative absorbance) of the CT absorption band and the growth of the aromatic cation radical; (b) temporal evolution of $\text{ArH}^{+\bullet}$ monitored at λ_{max} . Inset shows the first-order plot of the ion radical decay.

the maxima of the CT absorption bands of the series of anthracene complexes with the tropylium acceptor in acetonitrile solutions. [See Fig. 7(c)]. Accordingly the time-resolved spectra obtained from the tropylium-anthracene system relate directly to the charge-transfer excitation since there is no ambiguity about the adventitious local excitation of complexed (or uncomplexed) chromophores. Indeed, intense transient absorptions are observed in the visible region between 500 and 750 nm immediately following the CT excitation of the tropylium EDA complexes. Comparison with the steady-state absorption spectra of the corresponding anthracene cation radicals that are independently generated by the spectroelectrochemical technique (*vide supra*), establish the identity of the charge-transfer transients.

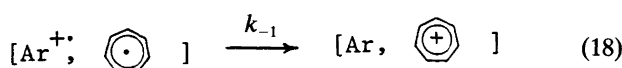
The appearance of the absorption spectra of the anthracene cation radicals is also accompanied by the disappearance of the charge-transfer absorption bands. The simultaneous nature of these spectral changes is clearly delineated in those anthracene donors with 9-phenyl, bromo, acetoxy and formyl substituents owing to the well-defined absorption maxima of their charge-transfer bands. Fig. 8(a) typically illustrates the growth of the aromatic cation radicals by the positive absorptions ($\Delta A > 0$) at wavelengths beyond 700 nm concomitant with the depletion of the ground-state EDA complexes by the negative CT absorptions ($\Delta A < 0$) at wavelengths less than 550 nm below the baseline. Such a photo-induced dismutation of the ground-state EDA complex readily identifies the charge-transfer excitation as in eqn. (17). The accompanying changes in the



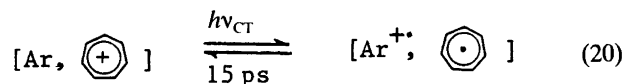
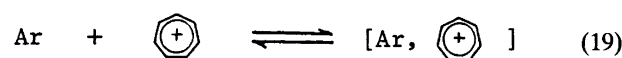
absorption spectra of the troyli cation and radical in eqn. (17) are obscured by their overlap with the dominant absorptions of the aromatic donors below 500 nm.

The time-resolved spectroscopic observation of $\text{Ar}^{+\bullet}$ ac-

companying the excitation of the charge-transfer band of the EDA complex accords with the electron promotion from the filled HOMO (or HOMO-1) of the arene donor Ar to the empty LUMO of the tropylium acceptor. The formation of arene cation radicals occurs within the rise-time of the 30 ps laser pulse. We conclude that the electron transfer from the arene donor to the tropylium acceptor in the EDA complex effectively occurs with the absorption of the excitation photon ($h\nu_{\text{CT}}$) in accord with Mulliken's theory. In the absence of any discernible charge-transfer photochemistry, the subsequent decay of the cation-radical absorbance in Fig. 8(b) derives from a dark (adiabatic) process. Since the observed first-order rate constants k_{-1} are too high to allow significant competition from diffusive separation, the annihilation of $\text{Ar}^{+\bullet}$ is ascribed to the reversal of the solvent-caged pair to regenerate the EDA complex [eqn. (18)]. The magnitudes of the driving force

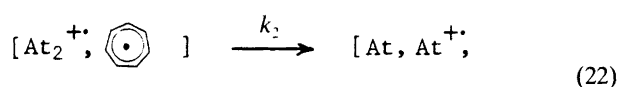
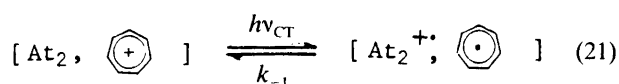


$-\Delta G_{\text{et}}$ for the back electron transfer in eqn. (18) are evaluated from the redox potentials E° of the anthracenes (At) and tropylium cation. In every case the driving force for the return of $\text{Ar}^{+\bullet}$ to the arene EDA complex is overwhelmingly large with $k_{-1} > 4 \times 10^{10} \text{ s}^{-1}$. The rapidity of the back electron transfer underlies the singular absence of productive photochemistry accompanying the continuous irradiation of the tropylium EDA complexes of various anthracene, naphthalene and benzene donors. Accordingly the photostationary state during charge-transfer excitation is schematically depicted as in Scheme 3.



Scheme 3.

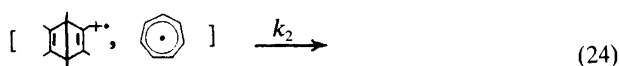
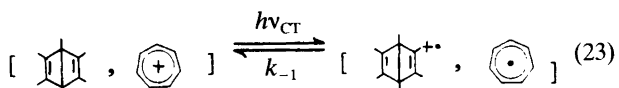
According to this formulation any photochemical transformation resulting from the CT excitation of the tropylium EDA complex is limited by the $\text{Ar}^{+\cdot}$ lifetime of $\tau \sim 15$ ps. Although these inextensible lifetimes discourage competition from any process involving the diffusive separation of the radical pair, the kinetics obstacle can be circumvented by a *unimolecular* process involving either the arene ion radical ($\text{Ar}^{+\cdot}$), the tropyli radical, or both in the solvent cage. Let us first consider the unimolecular fragmentation/rearrangement of $\text{Ar}^{+\cdot}$ as follows. The *cycloreversion of dianthracene* (At_2) is a direct consequence of populating the charge-transfer excited state of the tropylium EDA complex.²⁵ The photo-efficiency of this charge-transfer cycloreversion is limited by the unimolecular rate of fragmentation (k_2) of the dianthracene cation radical relative to back electron transfer [eqns. (21) and (22)]. The measured quantum yield of $\Phi_p = 0.02$ for the CT cycloreversion indicates that the rate constant k_{-1} for back electron trans-



Scheme 4.

fer in Scheme 4 [eqn. (21)] is ca. 10^{10} s^{-1} since the half-life of the dianthracene cation radical $\text{At}_2^{+\cdot}$ was previously estimated to be ca. 10^{-8} s .²⁶ Indeed the magnitude of k_{-1} for the back electron transfer in eqn. (21) evaluated by this indirect method is comparable to the values of k_{-1} obtained directly from the first-order decay of the arene cation radical.

The isomerization of hexamethyl Dewar benzene HMDB, like that of the dianthracene (*vide supra*), occurs as a direct consequence of the photoactivation of the tropylium EDA complex. Accordingly the charge-transfer mechanism for the aromatization of HMDB can be analogously presented as in Scheme 5. The preliminary evaluation of Φ_p



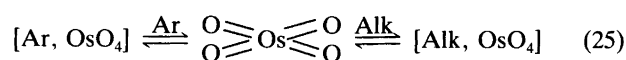
Scheme 5.

~ 4 suggests the participation of a chain process similar to the HMDB isomerization that Jones and coworkers reported earlier with other electron acceptors by both excited-state quenching and CT activation.²⁷ If so, an additional pathway involving the cation-radical chain process of the type proposed earlier²⁸ must be included in Scheme 5. Other photochemical studies directed at the interception of

such CT cation radicals by second-order processes have been unfruitful. For example, arene cation radicals are known readily to undergo both nucleophilic addition as well as deprotonation of methyl substituents.²⁹ In particular, the cation radicals of 9-methyl- and 9,10-dimethylanthracene are particularly stable, and they persist in the time-resolved studies of the CT excitation of the corresponding tropylium EDA complexes for rather prolonged times (*vide supra*). Attempts to intercept these methylarene cation radicals in the presence of added bases such as the hindered 2,6-di-*tert*-butylpyridine and 2,4,6-collidine lead to no change of the transient behavior; and the parent methylarenes are recovered intact even after prolonged CT irradiation. The more reactive cation radicals from hexamethylbenzene and 1,4-dimethylnaphthalene upon similar exposure yield no charge-transfer photochemistry, and yield neither products of nuclear addition nor side-chain deprotonation. Further attempts to intercept the transient anthracene cation radical formed by the charge-transfer excitation of the tropylium EDA complex in either acetic acid or methanol solution afforded no discernible photochemistry. Such trapping studies thus confirm the results arising from the direct observation of the CT transients by time-resolved picosecond spectroscopy. In order for effective CT photochemistry of arenes to occur via tropylium EDA complexes, a unimolecular process is required to compete effectively with $\text{Ar}^{+\cdot}$ lifetimes of ca. 15 ps. The latter largely precludes bimolecular quenching by second-order kinetics, except in those unusual cases such as the HMDB aromatization, in which leakage from the cage can be highly magnified by a subsequent chain process.

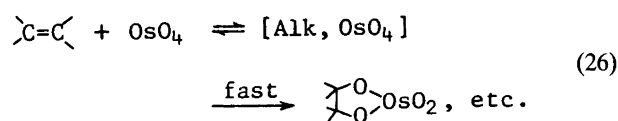
Electron-transfer activation in the thermal and photochemical osmylations of aromatic EDA complexes with osmium(VIII) tetraoxide

Oxo-metals have drawn increased attention as viable oxidation catalysts for various types of oxygen-atom transfers to organic and biochemical substrates.³⁰ However, only scant mechanistic understanding exists of the oxidation pathways, certainly with respect to the nature of the activation barrier and the identification of the reactive intermediate(s). Among oxo-metals, osmium tetraoxide is a particularly intriguing oxidant since it is known rapidly to oxidize various types of alkenes, but it nonetheless eschews the electron-rich aromatic hydrocarbons such as benzene and naphthalene.³¹ Such selectivities do not obviously derive from differences in the donor properties of the hydrocarbons since the oxidation (ionization) potentials of arenes are actually less than those of alkenes. The similarity in the electronic interactions of arenes and alkenes toward osmium tetraoxide relates to the series of electron donor-acceptor (EDA) complexes formed with both types of hydrocarbons [eqn. (25)].³²

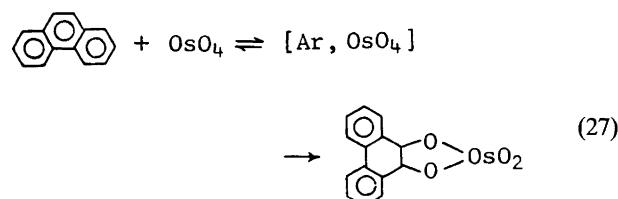


Common to both arenes and alkenes is the immediate appearance of similar colors that are diagnostic of charge-transfer (CT) absorptions arising from the electronic excitation ($h\nu_{CT}$) of the EDA complexes formed in eqn. (25). As such, the similarity in the color changes point to electronic interactions in the arene complex $[\text{Ar}, \text{OsO}_4]$ that mirror those extant in the alkene complex $[\text{Alk}, \text{OsO}_4]$.

The charge-transfer colors of the alkene EDA complexes are fleeting, and they are not usually observed owing to the rapid follow-up rate of osmylation [eqn. (26)]. By contrast, simple (monocyclic) arenes do not afford thermal adducts with osmium tetroxide, benzene actually being a most desirable solvent for alkene hydroxylation. However, with

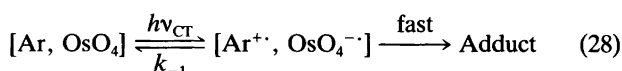


some extended polynuclear aromatic hydrocarbons such as benzo[a]pyrene, dibenz[a,h]anthracene and cholanthrene, a thermal reaction does lead to multiple osmate adducts and finally to polyhydric alcohols.³³ Tricyclic aromatic hydrocarbons such as phenanthrene show intermediate reactivity with osmium tetroxide to afford (over several weeks) the 1:1 adduct [eqn. (27)]. Osmylation in eqn. (27) occurs at



the HOMO site of the arene in a manner analogous to that observed in alkene osmylations [eqn. (26)]. In this context, anthracene is a particularly noteworthy substrate since it is purported to afford an unusual 2:1 adduct by oxidative attack at a terminal ring in preference to the most reactive *meso* (9,10-) positions.³⁴

We believe that the inextensible range of arene reactivities offers the unique opportunity to probe the mechanism of osmium tetroxide oxidations for four principal reasons. First, the EDA complexes in eqn. (25) relate alkenes directly to arenes via the oxo-metal interactions in the precursors relevant to oxidation. Second, the thermal osmylation of polynuclear arenes [see eqn. (27)] has an exact counterpart in the photostimulated osmylations that are widely applicable to even such otherwise inactive arenes as benzene. Since this charge-transfer process is readily associated with excitation ($h\nu_{CT}$) of the EDA complex to the ion pair [eqn. (28)] it is hereafter referred to



simply as charge-transfer osmylation. Third, the dual pathways of *thermal* and *charge-transfer* osmylation allow the regio- and stereo-chemistry for OsO_4 addition to be quantitatively compared, especially in the OsO_4 adducts of the polycyclic arenes: phenanthrene, anthracene and naphthalene. Fourth, the activation process or CT osmylation can be unambiguously established by the application of time resolved (picosecond) spectroscopy for direct observation of the reactive intermediates, as previously defined in other aromatic CT processes.^{7,10} Accordingly, our initial task in this study is to establish the common CT character of the EDA complexes of OsO_4 with the arene series: benzene, naphthalene and anthracene as well as the structural elucidation of their OsO_4 adducts by X-ray crystallographic and spectral analyses.

Aromatic EDA complexes with osmium(VIII) tetroxide. A colorless solution of osmium tetroxide in hexane or dichloromethane upon exposure to benzene turns yellow instantaneously.³⁵ With durene an orange coloration develops and a clear bright red solution results from hexamethylbenzene. The quantitative effects of the dramatic color changes are illustrated in Fig. 9 by the spectral shifts of the electronic absorption bands that accompany the variations

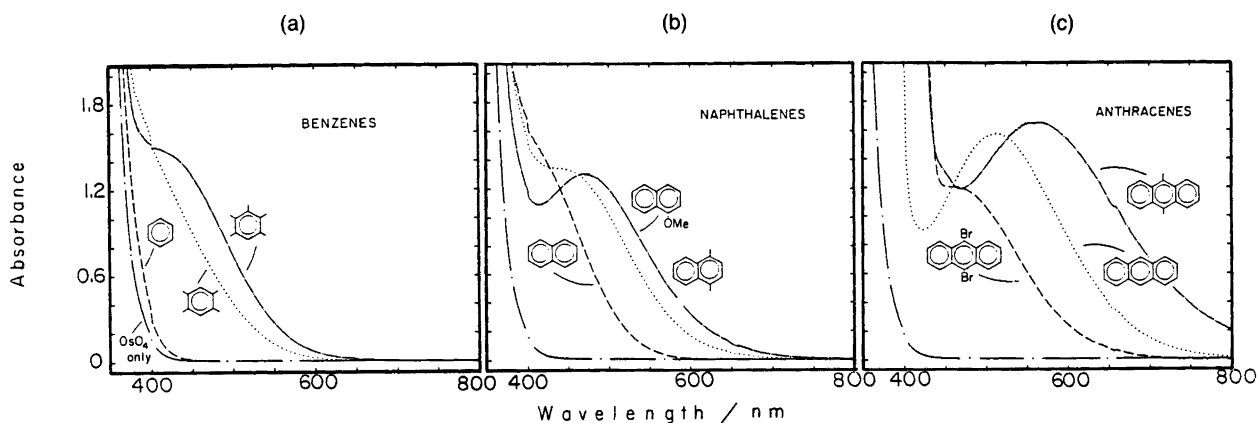
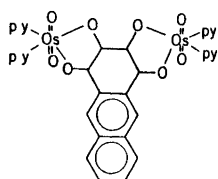
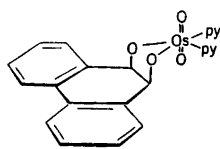


Fig. 9. Typical bathochromic shifts of the CT absorption bands of osmium tetroxide-EDA complexes with decreasing ionization potentials of arene donors: benzenes < naphthalenes < anthracenes.

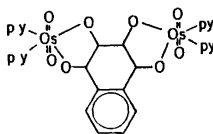
in aromatic conjugation and substituents. The progressive bathochromic shift parallels the decrease in the arene ionization potentials (E_i) in the order: benzene 9.23 eV, naphthalene 8.12 eV, anthracene 7.55 eV; much in the same manner as that observed with the tropylium acceptor in Fig. 7. Such spectral behavior is diagnostic of electron donor-acceptor complexes [Ar, OsO₄]. According to Mulliken, the new absorption bands derive from charge-transfer excitation with the energetics defined by $h\nu_{CT} = E_i - E_A - w_p^*$ (*vide supra*), where E_A is the electron affinity of the OsO₄ acceptor and w_p^* is the dissociation energy of the CT excited ion-pair state [Ar⁺, OsO₄⁻].



A



P



N

Thermal osmylation of naphthalene, anthracene and phenanthrene. Benzene shows no signs of osmylation in the absence of light, as indicated by the persistence of the yellow color of the [C₆H₆, OsO₄] complex in hexane even upon prolonged standing. On the other hand, the orange CT color of the phenanthrene complex [C₁₄H₁₀, OsO₄] slowly diminishes over a period of weeks, accompanied by the formation of a dark brown precipitate of composition (C₁₄H₁₀OsO₄). Dissolution of the solid in pyridine yields the 1:1 adduct (C₁₄H₁₀OsO₄py₂) **P** as the sole product in very low conversion. Anthracene behaves similarly to afford the 2:1 adduct in 10% conversion only after two months. The thermal osmylation can be expedited in a purple solution of refluxing heptane (100°C) to effect a 68% conversion in 30 h. However, even at these relatively elevated temperatures, naphthalene is converted into the corresponding 2:1 adduct to only a limited extent. In every case, the dark brown primary adducts are easily collected from the reaction mixture as insoluble solids, and then immediately ligated with pyridine for structural characterization. Indeed the characteristic IR and ¹H NMR spectra

of the anthracene, phenanthrene and naphthalene adducts **A**, **P** and **N**, respectively, allows the ready analysis of the osmylated adducts. Since these adducts are derived from the arenes with only OsO₄ present, the chemical transformation is hereinafter designated as the *direct thermal* or DT osmylation. For comparison, the same polynuclear arenes can be osmylated in the presence of promoter bases, typically pyridine. Under these conditions, the adducts **A**, **P** and **N** are formed directly in the reaction mixture and at substantially increased rates of reaction, as previously established with the related family of alkene substrates. Such a procedure differs visually from the DT osmylation described above in that the charge-transfer colors are not observed as transients, owing to the preferential complexation of OsO₄ with pyridine. Accordingly, this *promoted thermal* or PT osmylation is to be distinguished by the enhanced reactivity of the pyridine complex relative to the free OsO₄ in the DT osmylation. The corresponding increase in the yields of adducts such as **A**, **P** and **N** within a shorter span of reaction times is apparent from the comparison of the results of DT and PT osmylations.

Charge-transfer osmylation of benzene, naphthalene and anthracene. The various charge-transfer colors for the different arene complexes with OsO₄ are persistent for days. However when the colored solutions are deliberately exposed to visible light with energy sufficient to excite only the charge-transfer band, they always deposit a highly insoluble, dark brown solid of the OsO₄ adducts obtained from the direct thermal osmylation of arenes (*vide supra*). Since this photo-process must have arisen via the electronic excitation of the EDA complex, it is referred to hereafter as *charge-transfer* or CT osmylation for individual arenes. For example, the irradiation of the charge-transfer bands (see Fig. 9) of the OsO₄ complexes with various benzenes, naphthalenes and phenanthrene, yield the same osmylated adducts such as **N** and **P**, described above. Anthracene is unique in that it affords two entirely different types of products upon the photo-excitation of the EDA complex [C₁₄H₁₀, OsO₄] in dichloromethane and hexane, despite only minor solvent effects on the charge-transfer bands. Irradiation of the purple solution of anthracene and OsO₄ in dichloromethane at $\lambda > 480$ nm yields the 2:1 adduct **A** together with its *syn* isomer as the sole products. On the other hand, irradiation of the same purple-colored solution but in hexane under otherwise identical conditions leads to a small amount of polymeric osmium dioxide (OsO₂)_x. Work-up of the hexane solution yields anthraquinone as the major product contaminated with only traces (< 1%) of the 2:1 adduct **A**. Interestingly, even higher yields of anthraquinone are obtained from 9-bromo-, 9-nitro- and 9,10-dibromo-anthracene when the CT osmylation is carried out in hexane. Such an accompanying loss of the electronegative substituents (X = Br, NO₂) probably occurs via osmylation at the *meso* (9,10-) positions followed by oxidative decomposition of the unstable adduct with the stoichiometry of eqn. (29).

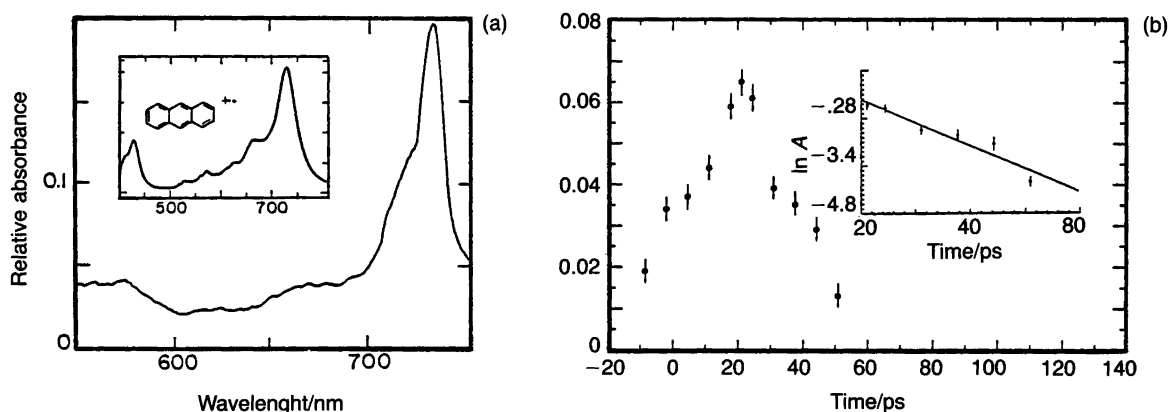
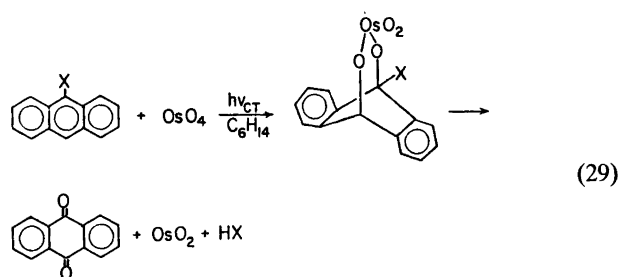


Fig. 10. Charge-transfer formation of transient ion radicals as described in Fig. 8, except for the use of osmium tetroxide as the acceptor in the EDA complexes with arenes (anthracene).



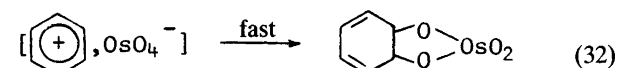
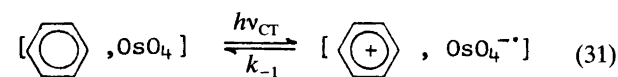
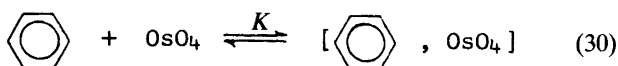
Time-resolved spectra of arene cation radicals in charge-transfer osmylation. In order to identify the reactive intermediates in the charge-transfer excitation of arene-OsO₄ complexes, the time-resolved spectra are measured immediately following the application of a 30 ps pulse consisting of the second harmonic at 532 nm of a mode-locked Nd³⁺:YAG laser. The wavelength of this excitation source corresponds to the maxima (or near maxima) of the charge-transfer absorption bands of the series of anthracene complexes with osmium tetroxide illustrated in Fig. 9(c). Accordingly, the time-resolved spectra from the anthracene-OsO₄ system relates directly to the CT osmylation since there is no ambiguity about either the adventitious local excitation of complexed (or uncomplexed) chromophores, or the photogeneration of intermediates that did not arise from the photoexcitation of the EDA complex. Indeed, intense absorptions are observed in the visible region between 700–800 nm from the excitation of the anthracene-OsO₄ complex, as shown in Fig. 10(a). This time-resolved absorption spectrum is obtained in the time interval of ca. 30 ps following the application of the 532 nm laser pulse. Comparison with the steady-state absorption spectrum of the anthracene cation radical (see inset) generated by the spectroelectrochemical technique, thus establishes the identity of the charge-transfer transient. Similar time-resolved spectra of arene cation radicals are obtained from various anthracene and naphthalene EDA complexes despite the excitation of only the low-energy tails of the CT bands in Fig. 9 with the 532 nm laser pulse. The evolution of the anthracene cation radical is followed by measuring

the absorbance change at $\lambda_{\text{max}} = 742 \text{ nm}$ upon the charge-transfer excitation of the EDA complex with a single laser shot of ca. 10 mJ. The time evolution of the absorbance shown in Fig. 10(b) includes the initial onset for ca. 30 ps owing to the rise time of the 30 ps (fwhm) laser pulse. The first-order plot of the decay portion is shown in the inset to the figure. Decay curves similar to those shown in Fig. 10 are also observed for the disappearances of the cation radicals derived from all of the other arene-OsO₄ complexes. In each case, the highest concentration can be obtained of the arene cation radical, the decays of which are all first-order processes. The magnitudes of the rate constant are applicable to the complete disappearance of Ar⁺, as indicated by the return of the cation-radical absorbances to the baseline.

Common features in thermal and charge-transfer osmylations. The [Ar, OsO₄] complexes are involved as the common precursors in the oxidative addition of osmium tetroxide to various arenes by the three independent procedures designated as direct thermal (DT), promoted thermal (PT) and charge-transfer (CT) osmylation. For example, the anthracenes react rather slowly with osmium tetroxide via the EDA complex to effect DT osmylation in non-polar solvents and afford 2:1 adducts that are then converted into the more tractable pyridine derivatives such as A. Alternatively, the same ternary product A is directly formed at a significantly *enhanced* rate by the PT osmylation of anthracene with a mixture of OsO₄ and pyridine. Finally, the OsO₄ adduct to anthracene is instantly produced by CT osmylation involving photoexcitation of the [Ar, OsO₄] precursor complex. As such, the three procedures represent different activation mechanisms for arene oxidation. Thus DT and PT osmylations are adiabatic processes in which the transition states are attained via the collapse of an arene donor with the OsO₄ and the base-coordinated OsO₄(py) electrophile, respectively. On the other hand, CT osmylation is a non-adiabatic process resulting from the vertical excitation of the [Ar, OsO₄] complex. For the latter, time-resolved picosecond spectroscopy can define

the relevant photophysical and photochemical events associated with the charge-transfer excitation of an arene EDA complex, as previously established with arene complexes involving other electron acceptors. Accordingly, the CT osmylation is delineated first and then related to DT and PT osmylation. Before proceeding, however, it is important to emphasize that the DT, PT and CT osmylations all share in common the formation of the 1:1 osmium(VI) cycloadduct ArOsO_4 in the initial rate-limiting step, since the concomitant loss of aromaticity produces a reactive alicyclic diene that is highly susceptible to further thermal osmylation.³¹ The universal adherence to the 2:1 adduct $\text{Ar}(\text{OsO}_4)_2$ (except phenanthrene), irrespective of the molar ratio of arene/ OsO_4 and the particular procedure employed, accords with the rapid addition of a second mole of OsO_4 in DT, PT and CT osmylations. This allows the focus on the formation of a single intermediate ArOsO_4 in order to delineate the unifying activation processes for DT, PT and CT osmylations.

Electron transfer in the charge-transfer osmylation of arenes. The direct observation of the reactive intermediates by the use of time-resolved picosecond spectroscopy and fast kinetics (Fig. 10) enables the course of CT osmylation to be charted in some detail. The analysis proceeds from the mechanistic context involving the evolution and metamorphosis of the CT ion pair, as summarized in Scheme 6 for the critical initial step [eqn. (32)] to form the 1:1 adduct

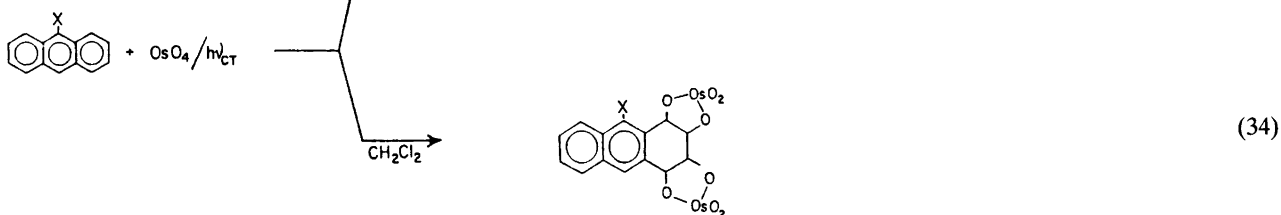
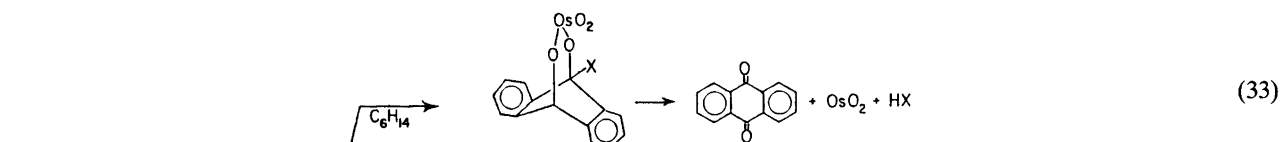


Scheme 6.

to a benzene donor, where the brackets denote solvent-caged pairs.

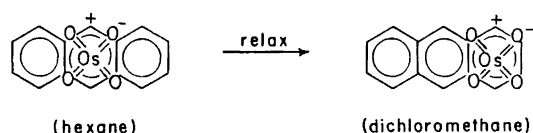
All the experimental observations on CT osmylation indeed coincide with the formulation in Scheme 6. Thus the exposure of arene to osmium tetroxide leads immediately to new absorption bands (Fig. 9) that are readily associated

with the formation of the EDA complex in eqn. (30). These binary complexes are always present in low steady-state concentrations owing to the limited magnitudes of K determined by the Benesi–Hildebrand method. The complexes are so weak that every attempt at isolation, including the freezing of various mixtures of OsO_4 in neat aromatic donors, merely lead to phase separation. The absorption bands are thus properly ascribed to contact charge transfer, as formulated by Orgel and Mulliken,³⁶ who predicted the CT absorption bands in these EDA complexes to be associated with the electronic excitation to the ion-pair state [eqn. (31)]. As such, the time-resolved spectrum in Fig. 10(a) identifies the formation of the arene cation radical to occur within the rise time of the 30 ps laser pulse. [The accompanying presence of the perosmate(VII) (OsO_4^-) counter-anion is obscured by the arene absorptions.] The electron transfer from the arene donor to the OsO_4 acceptor in the EDA complex eqn. (31) effectively occurs with the absorption of the excitation photon ($h\nu_{\text{CT}}$), in accord with Mulliken's theory. Furthermore the appearance at < 30 ps demands that Ar^+ and OsO_4^{--} are born as a contact (inner-sphere) ion pair with a mean separation essentially that of the precursor complex $[\text{Ar}, \text{OsO}_4]$ since this timescale obviates significant competition from diffusional processes. The seminal role of the ion pair $[\text{Ar}^+, \text{OsO}_4^{--}]$ as the obligatory intermediate from the photoexcitation of the EDA complex, must be included in any formulation of CT osmylation, by taking particular notice of how it decays. The spontaneous collapse of the CT ion pair in eqn. (32) represents the most direct pathway to arene cycloaddition – the measured half-life of $\tau \cong 35$ ps for the disappearance of the anthracene cation radicals in Fig. 10(b) largely precluding diffusive separation of such ion pairs. However the magnitudes of the product quantum yield $\Phi_p \sim 10^{-2}$ indicate that the primary route for ion-pair decay is the back electron transfer (k_{-1}) as the reverse step of eqn. (31). An energy-wasting process with an estimated rate constant of $k_{-1} \sim 10^{11} \text{ s}^{-1}$ derives from a highly exergonic driving force that is estimated to be $F\Delta E^\circ \cong -30 \text{ kcal mol}^{-1}$ based solely on the standard redox potentials of $E^\circ = +1.30$ and -0.06 V for anthracene and the perosmate (VII) anion, respectively. More relevant to this issue here is an estimated first-order rate constant for cycloaddition of $k_c = 10^9 \text{ s}^{-1}$ for the ion-pair collapse to the arene cycloadduct in Scheme 6. Such a relatively large rate constant also



points to a highly exergonic (bond-making) process for the cycloaddition in eqn. (32). Therefore the selectivity in adduct formation can be considered for various polynuclear arenes in which the initial addition of OsO₄ is possible at several sites. The regiospecificity observed in the CT osmylation of phenanthrene and 1,4-dimethylnaphthalene to produce only one isomeric adduct **P** and **N**, respectively accords with the reactive site centered on the arene HOMO. However in the extended polynuclear anthracenes, the separation of the HOMO and subjacent SHOMO (i.e., HOMO-1) is not so well delineated, and the regiospecificity is strikingly modulated by solvent polarity [eqns. (33) and (34)].

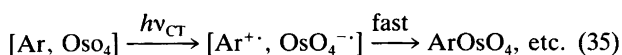
Ion-pair annihilation is known to occur with the greatest ease in highly non-polar alkanes.³⁷ Accordingly in hexane, the immediate collapse of the first-formed inner-sphere ion pair centered at the anthracene HOMO is expected to occur at the *meso* (9,10-) positions. Such an ion-pair collapse would produce anthraquinone in a manner similar to that presented in eqn. (29). On the other hand, the formation of *only* adduct **A** from the initial addition of OsO₄ to the terminal ring represents a very unusual regiospecificity insofar as other addition (and substitution) reactions of anthracene are concerned. It suggests that the initially formed HOMO ion pair (HIP) has time to relax in the more polar dichloromethane medium to the isomeric SHOMO ion pair (SIP) that rapidly leads to adduct **A**. This proposal receives support from the observation of adducts



related to **A** from the CT osmylation of both 9-methyl- and 9,10-dimethyl-anthracene in *hexane*. The enhanced stability of the cation radicals from these relatively electron-rich anthracenes will optimize the opportunity to convert the HIP into the more reactive SIP even in the non-polar hexane medium, particularly if the collapse of the former were reversible.

Electron transfer as the common theme in arene osmylation.

The wide-ranging reactivity of various aromatic hydrocarbons to OsO₄ offers a unique opportunity to probe the activation process for oxidative osmylation, especially with regard to the role of the EDA complex and the reactive intermediates. In particular, the deliberate photoexcitation ($h\nu_{CT}$) of the EDA complex in hexane or dichloromethane effectively activates various arenes including benzenes, naphthalenes and anthracenes to CT osmylation. This photoactivated process is readily associated with the charge-transfer ion pair [eqn. (35)] as established by the growth



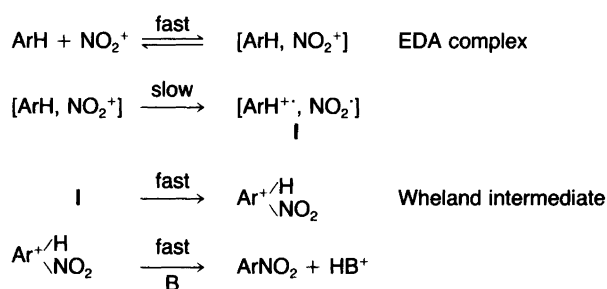
and decay of arene cation radicals with the aid of time-resolved picosecond spectroscopy. When kept in the dark, the same solutions of the EDA complexes slowly afford arene-OsO₄ adducts that are identical with those derived by CT osmylation. Indeed the close kinship between the thermal and charge-transfer activation of osmylation is underscored by the unique adduct **A** in which OsO₄ addition occurs exclusively to the terminal ring and not to the usual *meso* (9,10-) positions of anthracene. The activation process to form the related adiabatic ion pair [Ar^{·+}, OsO₄^{·-}] in the thermal osmylation provides the unifying theme in arene oxidation. Furthermore the promoted thermal osmylation of arenes via the 5-coordinate pyridine analogue OsO₄py is related to the widely used procedure for alkene bis-hydroxylation and the same regiochemistry observed, especially with anthracene donors, indicates that the activated complex for PT osmylation is strongly related to that for DT osmylation.

The variable regiochemistry observed in the collapse of [Ar^{·+}, OsO₄^{·-}] to the cycloadduct ArOsO₄ underscores the importance of the contact (inner-sphere) ion pair structure in determining the course of electron-transfer oxidation. Since such structures are not readily determined as yet, the structural effects induced by qualitative changes in solvent polarity, salts, additives, and temperature are reaction variables that must always be optimized in the synthetic utilization of electron-transfer oxidation by either thermal or photochemical activation.

Aromatic EDA complexes in nuclear nitration

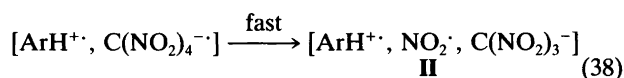
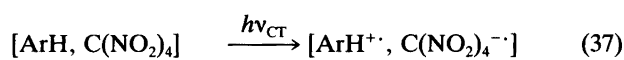
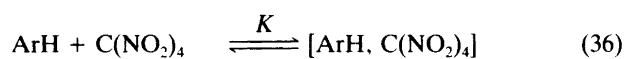
The idea that charge transfer may play a key role in aromatic nitration with nitronium ion was first suggested in 1945 by Kenner,³⁸ who envisaged an initial step that 'involves transference of a π -electron.' Later Brown³⁹ postulated charge-transfer complexes as intermediates, and Nagakura⁴⁰ provided further theoretical support for one-electron transfer between an aromatic donor (ArH) and an electrophile such as NO₂⁺. Despite notable elaborations by Pederson,⁴¹ Perrin,⁴² Ebersson and Radner,⁴³ and others, this formulation has not been widely accepted for nitration and related electrophilic aromatic substitutions.⁴⁴

As broadly conceived, the seminal question focuses on the activation process(es) leading up to the well-established Wheland or σ -intermediate.⁴⁵ In the electron-transfer mechanism, the formation of the ion radical pair **I** is the distinctive feature, as summarized in Scheme 7. Accordingly, the properties and behavior of the intimate ion radical pair **I** are crucial to establishing its relationship with the numerous facets⁴⁶ of electrophilic aromatic nitration. For these reasons it is especially important to know whether **I** will actually lead to the appropriate Wheland intermediate, and in the amounts necessary to establish the isomer distributions commonly observed in aromatic nitrations. However, the independent proof of the ion radical pair **I** has not been forthcoming owing to its expectedly transitory character.



Scheme 7.

Charge-transfer nitration of aromatic donors. Picosecond time-resolved spectroscopy has defined the relevant photophysical and photochemical processes associated with the charge-transfer excitation of an arene complex such as anthracene with tetranitromethane.¹⁰ As applied to benzenoid donors ArH, the formation of the pertinent ion radical pair by charge-transfer excitation is summarized in Scheme 8. All the experimental observations with various ben-



Scheme 8.

zenoid donors and tetranitromethane indeed coincide with the formulation in Scheme 8. Thus the exposure of ArH to a nitrating agent such as TNM as in Fig. 11 leads immediately to the EDA complex in eqn. (36). It is singularly

noteworthy that the charge-transfer spectrum of the aromatic EDA complex with TNM is not fundamentally distinguished from the CT spectra of other common nitrating agents shown in Fig. 11. Moreover, all of these EDA binary complexes are present in low steady-state concentrations owing to the limited magnitude of K as measured by the Benesi-Hildebrand method. Activation of the EDA complex by the specific irradiation of the CT band results in a photoinduced electron transfer in accord with Mulliken theory. Thus the irreversible fragmentation following the electron attachment to TNM leads to the ion radical pair II in eqn. (38) (see Fig. 12). The measured quantum yield of $\Phi \cong 0.5$ is similar to that ($\Phi \cong 0.7$) obtained for anthracene. Such high quantum yields relate directly to the efficiency of ion radical pair production in eqn. (38) relative to energy wastage by back electron transfer in eqn. (37). Moreover the short lifetime (< 3 ps) of $\text{C}(\text{NO}_2)_4^{\cdot-}$ ensures that ArH^+ and $\text{NO}_2^{\cdot-}$ are born as an ion radical pair, initially trapped within the solvent cage, since this time-scale obviates any competition from diffusional processes.¹⁰

Charge-transfer excitation thus provides the experimental means of generating the intimate ion radical pair $[\text{ArH}^+, \text{NO}_2^{\cdot-}]$ for Scheme 7 in sufficient concentrations and in a discrete electronic state as well as geometric configuration. Coupled with the observation of the fast kinetics allowed by the use of laser-flash photolytic techniques, we now focus on the pathway by which the ion radical pair collapses to nitration products with two series of aromatic ethers.

Dimethoxybenzenes as the aromatic donors in nitration. *p*-Dimethoxybenzene (DMB) is the prototypical electron-rich aromatic donor owing to its reduced oxidation potential of only 1.30 V vs. SCE. Charge-transfer excitation of the 1:1 DMB complex with TNM proceeds quantitatively

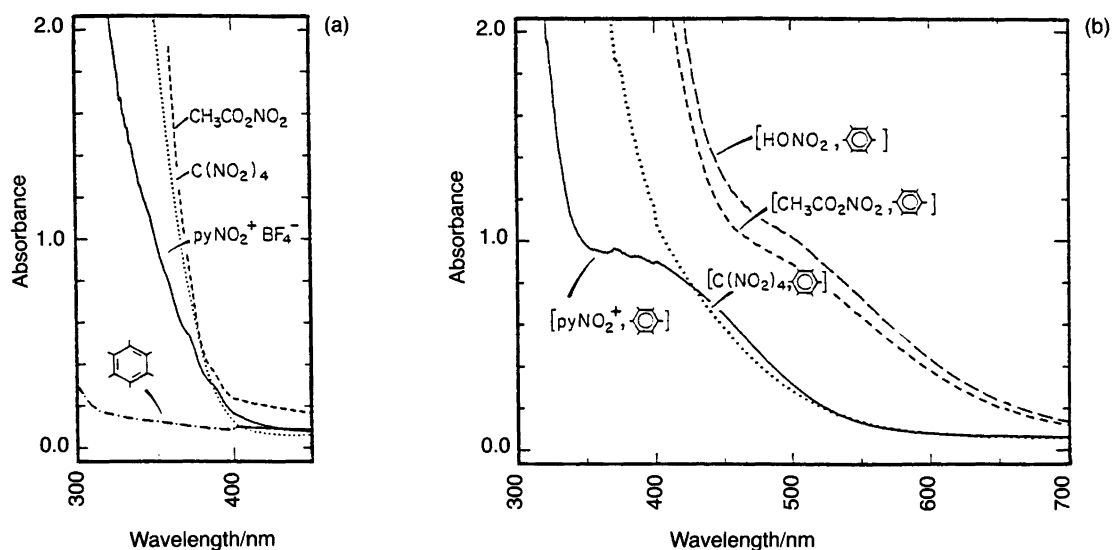


Fig. 11. (a) Comparative charge-transfer spectra of hexamethylbenzene-EDA complexes with various nitrating agents as indicated; (b) absorption spectra of the uncomplexed donor and acceptors.

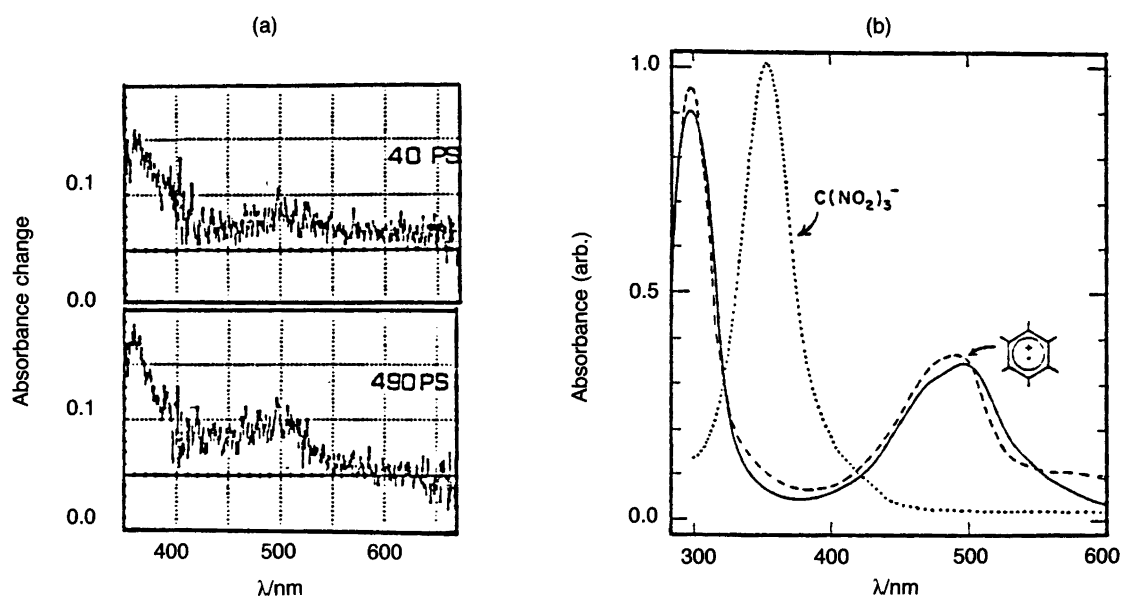
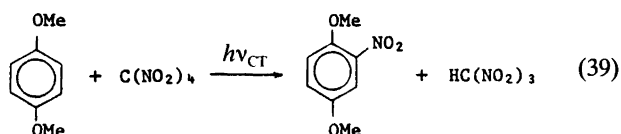
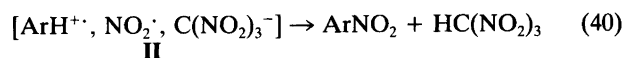


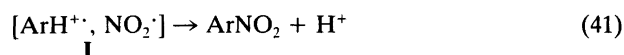
Fig. 12. (a) Time-resolved ps absorption spectra at 40 and 490 ps following the 532 nm laser pulse of the hexamethylbenzene-EDA complex with tetranitromethane; (b) absorption spectra of HMB^{•+} generated spectroelectrochemically and of C(NO₂)₃⁻ obtained from the tetrabutylammonium salt.



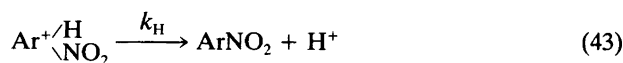
according to the stoichiometry, given in eqn. (39). The photochemical process is hereafter referred to as *charge-transfer nitration*. The excellent material balance obtained in charge-transfer nitration of DMB demands that the ion radical pair **II** in Scheme 8 proceeds quantitatively to the nitration products according to the stoichiometry of eqn. (40).



Such a transformation must occur spontaneously with no discrimination among the reactive intermediates to accord with the absence of a deuterium kinetic isotope effect. The latter is not consistent with the collapse of **II** as an ion pair [ArH^{•+}, C(NO₂)₃^{•-}] by proton transfer to the very weakly basic trinitromethanide. Furthermore, the presence of extra trinitromethanide (deliberately added as the tetrabutylammonium salt TBAT) exert essentially no influence on either the course or the kinetics. Accordingly the trinitromethanide is merely an innocuous by-stander insofar as the conversion of the ion pair **II** in eqn. (40) is concerned. It follows that the disappearance of the arene ion radical must be directly related to its interaction with NO₂^{•-} [eqn. (41)].



Indeed such cation radicals have been prepared from various arenes by other experimental methods, especially electrochemical oxidation.²⁶ The arene cation radicals related to DMB^{•+} are weak Brønsted acids, but they are highly susceptible to nuclear addition, *vide infra*,^{26,47} (Scheme 9).

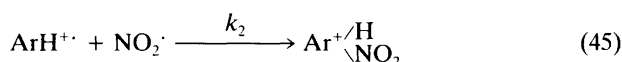
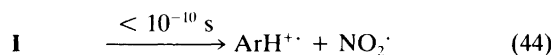


Scheme 9.

The σ -adduct in eqn. (42) is the Wheland intermediate in electrophilic nitration, which is known to show no deuterium kinetic isotope effect for k_{H} upon deprotonation in eqn. (43).⁴⁸ According to Scheme 9 formation of the various isomeric Wheland intermediates will occur from the collapse of the ion radical pair in eqn. (42). Consequently the isomer distributions in the nitration products relate directly to the relative rates of addition to the various nuclear positions provided that it is irreversible and/or the adduct deprotonates rapidly. Thus the strong correlation observed between the spin densities at the various nuclear positions of ArH^{•+} and the isomeric product distribution in aromatic nitration⁴⁹ bears directly on the mechanism of such an ion radical pair collapse to the Wheland intermediate.

Although the Wheland intermediate in Scheme 9 has not been separately observed, the time-resolved spectral changes of the cation radical ArH^{•+} do provide insight as to how it is formed. Thus the relatively long lifetime of the

rather stable arene cation radical $\text{DMB}^{+\cdot}$ is sufficient to allow diffusive separation of the ion radical pair **I** to $\text{ArH}^{+\cdot}$ and $\text{NO}_2^{\cdot-}$ as essentially 'free' species.²⁶ The second-order process with the rate constant k_2 for the disappearance of $\text{DMB}^{+\cdot}$ then represents the 'recombination' of these separated species to form the Wheland intermediate (Scheme 10).

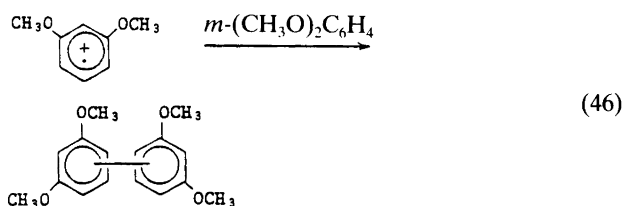


Scheme 10.

The strong solvent dependence of k_2 is largely attributed to the stabilization of $\text{ArH}^{+\cdot}$ by solvation, since it decreases with increasing solvent polarity in the order: hexane > benzene > dichloromethane. The slight negative salt effect on k_2 also accords with this conclusion. Since the common-ion salt TBAT has no effect on the charge-transfer nitration of DMB, the trinitromethanide is not a sufficiently strong nucleophile to intercept the associated cation radical $\text{DMB}^{+\cdot}$ in a process which would be tantamount to ion pair collapse of **II**. However it has been shown in electrophilic nitration that the Wheland intermediate can be efficiently captured by a built-in nucleophile, usually a carboxylic acid, and the nitration product isolated as an *ipso* adduct.⁵⁰

Aromatic nitration via the ion radical pair **I** in eqn. (41) thus proceeds with high efficiency when it is induced by the charge-transfer excitation of arene-TNM complexes. Furthermore the yields and isomeric distributions among the nitration products from various dialkoxybenzenes are strikingly akin to those obtained under the more conventional electrophilic conditions.⁵¹ One can conclude from these observations that intermediates leading to the conventional electrophilic nitration are similar to, if not the same as, those derived by charge-transfer nitration. Indeed the parallel behavior extends even to those arenes in which significant amounts of by-products are formed. For example, the direct nitration of *m*-dimethoxybenzene is reported to produce 2,4-dimethoxynitrobenzene in only poor yields

(~30%).⁵² In addition, an unusual blue coloration develops rapidly during the electrophilic nitration of *m*-dimethoxybenzene. The same intense blue color occurs with *m*-dimethoxybenzene and TNM, but only upon deliberate exposure of the EDA complex to CT irradiation. Among the dimethoxybenzenes, the *meta* isomer is unique in that it is the only one to develop an intense (blue) coloration upon electrophilic and/or charge-transfer nitration. The subsequent chromatography of the highly colored reaction mixture from electrophilic nitration yields significant amounts of dimethoxyphenyl dimers which are known to derive from the cation radical by arene coupling and similar re-



sults are observed with 2,6-dimethoxytoluene and 1,3,5-trimethoxybenzene.

Haloanisoles as the aromatic donors in nitration. The anisoles (XA) with 4-fluoro, chloro and bromo substituents are substantially poorer electron donors as evidenced by their oxidation potentials E_{ox}° that are ca. 500 mV more positive than that of DMB (*vide supra*). As a result, the corresponding cation radicals $\text{XA}^{+\cdot}$ are significantly more susceptible than $\text{DMB}^{+\cdot}$ to nucleophilic addition. The latter can be circumvented in the CT nitration of haloanisoles by either the addition of neutral salt in dichloromethane or the use of acetonitrile as a polar medium. Most importantly the decay of the transient cation radical $\text{XA}^{+\cdot}$ formed by the CT excitation of the EDA consistently followed *first-order* kinetics. The clean first-order rate processes are applicable to the complete disappearance of $\text{XA}^{+\cdot}$ as established by the return of the absorbance to the baseline in Fig. 13 for X = Cl. Since only CT nitration of XA occurs under these experimental conditions, the experimental

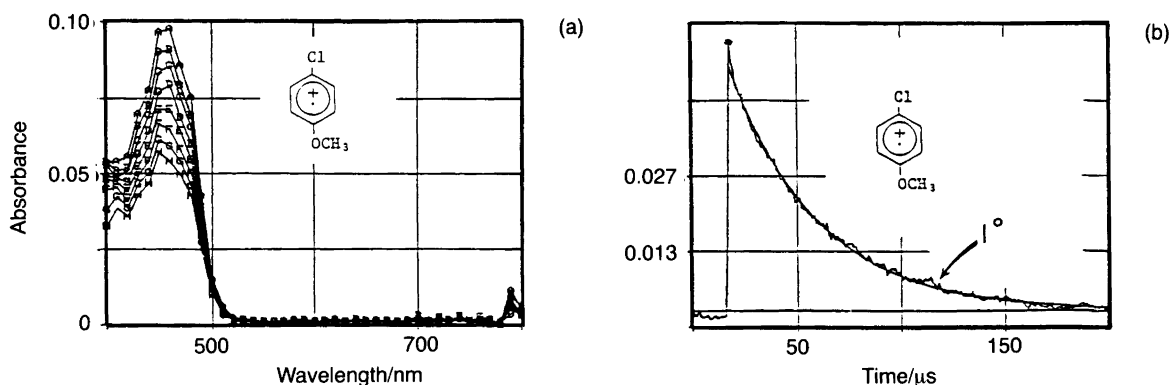
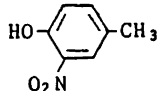
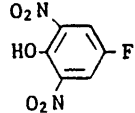
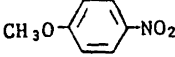
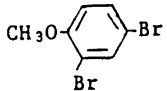


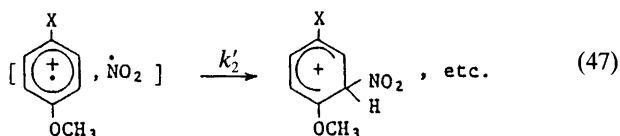
Fig. 13. (a) Time-resolved absorption spectrum of the donor cation radical following the CT excitation of the tetranitromethane complex with arene (*p*-chloroanisole); (b) first-order decay of the donor cation radical to the Wheland intermediate in aromatic nitration.

Table 2. Aromatic products from the electrophilic (E) and charge-transfer (ET) nitration of anisole derivatives.^a

Substituent in anisole		Aromatic products (mol %)					
		2-NO ₂	3-NO ₂	4-NO ₂	5-NO ₂	6-NO ₂	Others
None	{ ET	35	3	43	—	—	
	{ [E]	[31]	[2]	[67]			
2-CH ₃	{ ET	—	—	68	—	32	
	{ [E]			[60]		[40]	
4-CH ₃	{ ET	60	—	—	—	—	
	{ [E]	80					
4-F	{ ET	83	—	—	—	—	
	{ [E]	100					
4-Br	{ ET	42	—	—	—	—	
	{ [E]	48					
							
							20 [25]

^aET = electron transfer C(NO₂)₄/hν_{CT} and [E] = electrophilic HNO₃/Ac₂O or HNO₃/H₂SO₄, 0 °C.

first-order rate constant k_2 relates solely to the nuclear collapse of the ion radical pair [eqn. (47)]. Indeed the regioselectivity of such an ion radical pair collapse yields the isomeric mixture of nuclear nitration products that is essentially indistinguishable from that obtained under con-



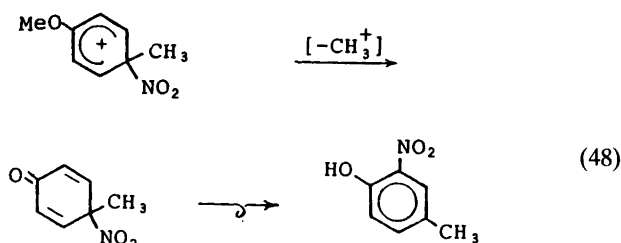
ventional electrophilic conditions (Table 2). It is also worth noting that the by-products from CT nitration in Table 2 are strongly reminiscent of the by-products reported in electrophilic nitration of the anisoles with nitric acid. In particular, the demethylation of the methoxy group to afford nitrophenols, and the trans-bromination of 4-bromoanisole to afford a mixture of 4-nitroanisole and 2,4-dibromoanisole are both symptomatic of radical-pair collapse at the *ipso* positions. These produce the σ -adducts which are akin to the Wheland intermediates known to undergo such transformations [eqns. (48) and (49)].⁵³

Structural variation in the kinetics of ion radical pair collapse. The kinetics of the collapse of the ion radical pair [ArH⁺, NO₂[·]] from the representative arenes is summarized in Table 3. The decay of the spectral transients for nitration in eqn. (42) is a reflection of the stability of the aromatic cation radical. For example, the cation radical from *p*-methylanisole decays by second-order kinetics similar to the kinetic behavior of the long-lived cation radical from *p*-methoxyanisole. The large difference in the rates of diffusive combination with NO₂[·] in Table 3 (see column 4) corresponds to their relative stabilities as measured by $\Delta E^\circ \equiv 8.5 \text{ kcal mol}^{-1}$ of the parent arenes (column 1). There is a further, larger gap of $\Delta E^\circ \equiv 10.4 \text{ kcal mol}^{-1}$ which separates the stabilities of the cation radicals of *p*-methylanisole and *p*-fluoroanisole, the least reactive haloanisole. Strikingly, every member of the family of *p*-haloanisole cation radicals reacts with NO₂[·] by first-order kinetics. This decay pattern strongly suggests that the CT nitration occurs by the cage collapse of the geminate radical pair [ArH⁺, NO₂[·]] prior to diffusive separation, except when the anisole cation is a relatively stabilized species such as those with *p*-methyl and *p*-methoxy substituents.

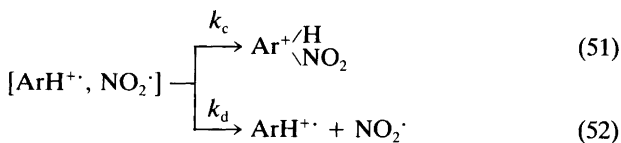
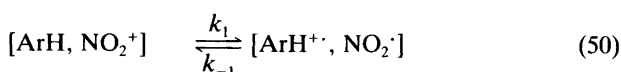
Table 3. Kinetics of the charge-transfer nitration of substituted anisoles.^a

E°/V vs. SCE	4-X-C ₆ H ₄ -OCH ₃ X	Kinetics order	Rate constant ^b
1.30	Methoxy	2°	1.0 × 10 ⁴
1.67	Methyl	2°	2.5 × 10 ⁵
2.12	Fluoro	1°	1.9 × 10 ⁴
2.00	Chloro	1°	2.4 × 10 ⁴
1.78	Bromo	1°	3.7 × 10 ⁴

^aIn units of A⁻¹ s⁻¹ for second-order and s⁻¹ for first-order kinetics. ^bValues of k_2' (see text).



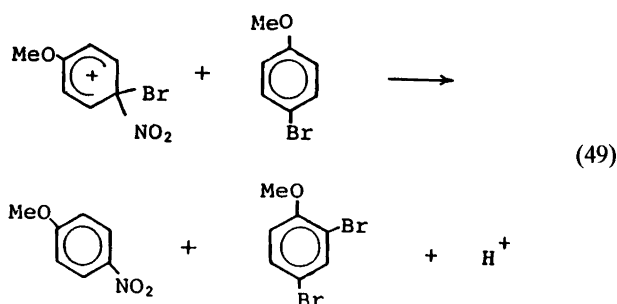
ion radical pair is manifested by its diffusive separation. Scheme 11 presents this construct in a kinetics context.⁴⁴



Scheme 11.

(i) The extent to which $k_d \gg k_c$ allows side reactions to compete as a result of the diffusive separation of ArH^+ and NO_2^- . The experiments with aromatic diethers clearly belong in the latter category since the evolution of nitration products takes place in the $\mu\text{s}/\text{ms}$ time regime. Nonetheless the diffusive recombination of ArH^+ and NO_2^- pairs with the second-order rate constant k_2 can occur in eqn. (45) with very high efficiency. The competition from diffusion is represented by the intermolecular trapping of ArH^+ in eqn. (46).

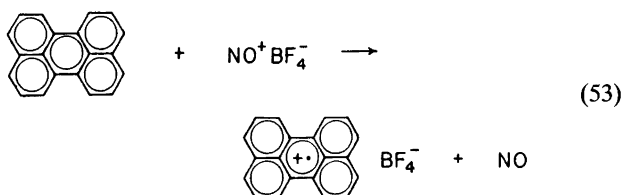
(ii) The efficient collapse of the ion radical pair to the Wheland intermediate is represented by $k_c \gg k_d$. Such a direct collapse of the ion radical pair has its counterpart in CT nitration by the observed first-order decay of the spectral transients derived from the 4-haloanisole donors (compare Fig. 13). Indeed the clean first-order rate constants k_2' listed in Table 3 for the ion radical pair collapse in eqn. (47) relate to the rate constant k_c in eqn. (51) of Scheme 11. However the magnitude of $k_2' \sim 10^4 \text{ s}^{-1}$ is at least six orders of magnitude lower than that expected from the diffusional correlation times of 10^{-10} – 10^{-11} s. In other words, if k_2' measures the cage collapse of the initial ion radical pair formed by the CT excitation in eqn. (37), then how can it avoid diffusive separation prior to the formation of the Wheland intermediate? In order to address this important point, we turn to the time-resolved studies of aromatic EDA complexes with NO^+ as a cationic electrophile related to NO_2^+ .⁵⁴ [Note that the thermal reactions of NO_2^+ occur too rapidly to allow the aromatic EDA (precursor) complexes to be examined separately.]



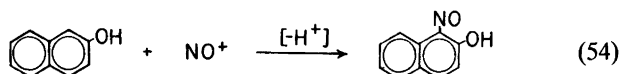
Comments on the mechanism of aromatic nitration. The foregoing results underscore the strong similarity between electrophilic and charge-transfer nitration of aromatic ethers, with regard to both the nitration products and the aryl by-products. Since the latter is symptomatic of arene cation radicals, the parallel does extend to some reactive intermediates in common. As such, the most economical formulation for electrophilic nitration would also include a pathway which is common to charge-transfer nitration, namely, via the ion radical pair I, as presented in Scheme 7. This mechanism differs from the conventional formulation in which the $[\text{ArH}, \text{NO}_2^+]$ pair is directly converted into the Wheland intermediate in a single step, rather than via the ion radical pair I. Previous studies have established the strong similarity in the activation barriers (i.e., energetics) for these two processes.⁴⁹ Accordingly the problem can be considered in an alternative framework, namely, the lifetime of the ion radical pair. At one extreme of a very short lifetime, the inner-sphere ion radical pair is tantamount to the transition state for the concerted one-step process. At the other extreme of a very long lifetime, the outer-sphere

Aromatic EDA complexes with nitrosonium ion

A nitrosonium salt like a nitronium salt can serve effectively either as an oxidant or as an electrophile toward different aromatic substrates. Thus the electron-rich polynuclear arenes suffer electron transfer with $\text{NO}^+ \text{BF}_4^-$ to afford stable arene cation radicals⁵⁵ [eqn. (53)]. Other acti-



vated aromatic compounds such as phenols, anilines and indoles undergo nuclear substitution with nitrosonium species⁵⁶ [eqn. 54] that are usually generated *in situ* from the



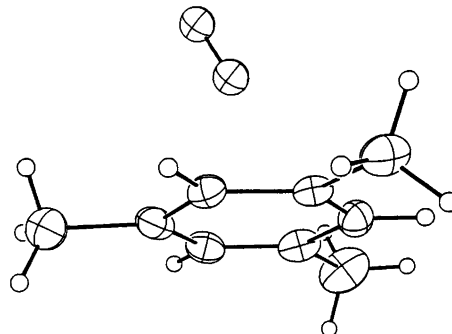
treatment of nitrites with acid. It is less well known, but nonetheless experimentally established,⁵⁷ that NO^+ forms intensely colored charge-transfer complexes with a wide variety of common arenes (ArH) [eqn. (55)]. For example,



benzene, toluene, xylenes and mesitylene generate yellow to orange vivid hues when added to colorless solutions of $\text{NO}^+ \text{PF}_6^-$ in acetonitrile. Analogously, the more electron-rich durene, pentamethylbenzene, hexamethylbenzene and naphthalene afford dark red solutions when exposed to NO^+ (Fig. 14). These charge-transfer colors are sufficiently persistent to allow single crystals of various arene CT complexes with NO^+ to be isolated for structural elucidation by X-ray crystallography.⁵⁸

Molecular structures of the aromatic EDA complexes with NO^+ . Although $\text{NO}^+ \text{PF}_6^-$ is insoluble in dichloromethane, it dissolves readily when an arene donor is present. These highly colored solutions, when allowed to stand at -20°C ,

deposit crystals of the CT complexes. In this manner, the 1:1 arene complexes $[\text{ArH}, \text{NO}^+ \text{PF}_6^-]$ are isolated with $\text{ArH} =$ mesitylene, durene, pentamethylbenzene and hexamethylbenzene. The ORTEP diagram from the X-ray crystallography of the mesitylene complex presented below⁵⁹



accords with those previously isolated by Brownstein and coworkers from liquid sulfur dioxide.⁵⁷ Indeed the relevant CT interaction clearly derives from the centrosymmetric (η^6) structure of the arene- NO^+ pair reminiscent of the other aromatic EDA structures presented in Fig. 4. However, the NO^+ complexes are unusual in two important ways. First, the formation constant K in Table 4 is strongly dependent on the donor strength (i.e., ionization potential) for the arene – increasing dramatically from 0.5 M^{-1} with benzene to $31\,000 \text{ M}^{-1}$ with hexamethylbenzene (HMB).⁶⁰ Second, the frequency of the N–O stretching band in the infrared spectrum decreases markedly from $\nu_{\text{NO}} = 2037 \text{ cm}^{-1}$ in the toluene complex to $\nu_{\text{NO}} = 1880 \text{ cm}^{-1}$ in the

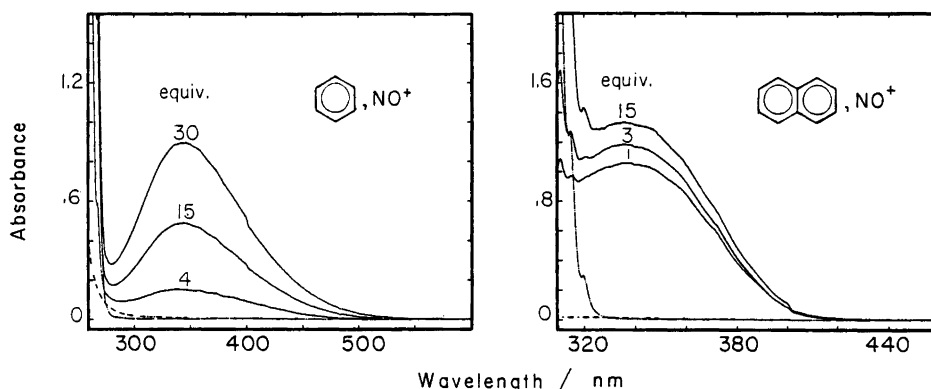


Fig. 14. Typical charge-transfer absorption spectra of nitrosonium EDA complexes with arenes (benzene and naphthalene).

Table 4. Formation constants of arene charge-transfer complexes with NO^+ .^a

Arene	10^{-3} M^b	E_i/eV	$\text{NO}^+\text{BF}_4^-/10^{-3} \text{ M}$	$\lambda_{\text{CT}}/\text{nm}$	K/M^{-1}	$\epsilon_{\text{CT}}/\text{M}^{-1} \text{ cm}^{-1}$
Benzene	(41–580)	9.23	9.8	346	0.46	780
Toluene	(45–75)	8.82	6.0	342	5.0	400
Mesitylene	(3.2–23)	8.42	0.81	345	56	2080
1,3,5-Tri- <i>tert</i> -butylbenzene	(3.3–19)	8.19	0.92	349	34	1730
Pentamethylbenzene	(2.7–15)	7.92	0.20	337	5100	2400
Hexamethylbenzene	(0.15–17)	7.71	0.20	337	31,000	3000

^aIn acetonitrile at 25°C . ^bLower–upper concentration range.

Table 5. Infrared spectra of arene CT complexes with $\text{NO}^+ \text{PF}_6^-$.

[ArH, $\text{NO}^+ \text{PF}_6^-$] ArH	Solid/ cm^{-1} NO^+ (fwhm) ^b	Δ^c	Solution/ cm^{-1} NO^+ (fwhm)
Hexamethylbenzene	1899 (152)	441	1880 (49)
Pentamethylbenzene	1927 (196)	413	1904 (59)
Durene	1986 (191)	355	1929 (60)
Mesitylene	2016 (157)	324	1967 (93)
<i>p</i> -Xylene	^d		1998 ^e (92)
<i>o</i> -Xylene	^d		2000 ^e (97)
Toluene	2042 ^f (180)	298	2037 ^e (91)

^aIn dichloromethane. ^bFull-width half maximum. ^cShift from free $\text{NO}^+ \text{PF}_6^-$ at 2340 cm^{-1} . ^dNot measured. ^eIn nitromethane. ^fGround mixture of toluene with $\text{NO}^+ \text{PF}_6^-$.

hexamethylbenzene complex (Table 5). Such a large change in ν_{NO} parallels the difference between the uncomplexed acceptor [$\nu(\text{NO}^+) = 2280 \text{ cm}^{-1}$] and free nitric oxide [$\nu(\text{NO}) = 1876 \text{ cm}^{-1}$].

The unusually pronounced dependence of both the formation constant K and N–O stretching frequency of the aromatic EDA complexes with NO^+ is illustrated in Fig. 15. Indeed the strong correlations with the aromatic donor strength as evaluated by the ionization potential point to a sizeable change in the charge-transfer component in the ground state of these complexes.⁶¹ In particular, the value of ν_{NO} in the hexamethylbenzene (HMB) complex, which is essentially the same as that of free NO, suggests complete electron transfer in the ground state.⁶²

According to Mulliken theory,¹⁴ the ground state of weak EDA complexes (with K typically $< 10 \text{ M}^{-1}$) can be described by eqn. (56) with the coefficients $a \gg b$ to denote

$$\psi = a \psi_{\text{D,A}} + b \psi_{\text{D}^+\text{A}^-} \quad (56)$$

a minor contribution from the charge-transfer state.⁶³ The complete reversal upon CT excitation generates an excited state with a large (total) contribution from the charge-transfer state [eqn. (57)]. Indeed, the time-resolved spec-

$$\psi^* = b \psi_{\text{D,a}} - a \psi_{\text{D}^+\text{A}^-} \quad (57)$$

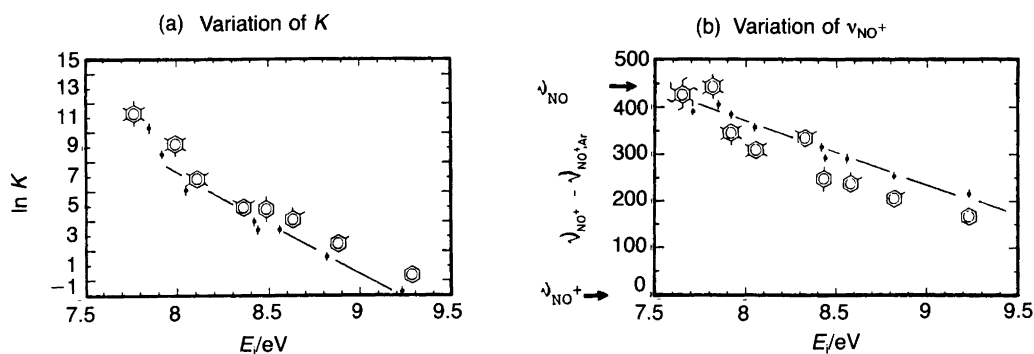


Fig. 15. Variations of (a) the formation constant K and (b) the N–O stretching frequencies ($\nu_{\text{NO}^+} - \nu_{\text{NO}^+, \text{Ar}}$) in the infrared spectra of 1:1 EDA complexes of NO^+ and various arenes as indicated.

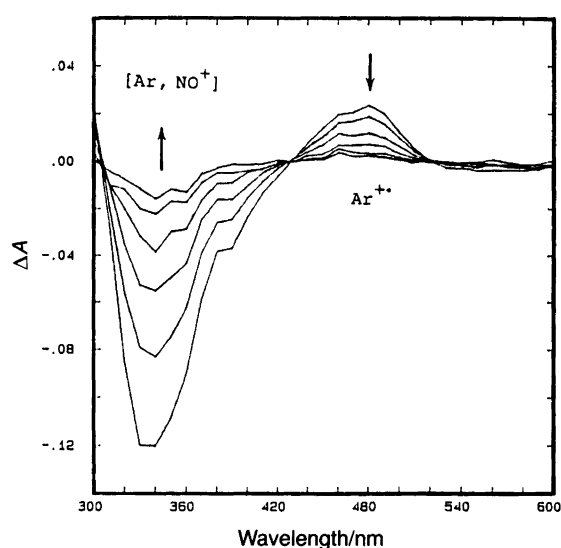


Fig. 16. Typical time-resolved absorption spectrum following the CT excitation of nitrosonium EDA complexes with arene (hexamethylbenzene) showing the bleaching of CT absorption and growth of the donor cation radical (HMB^+).

troscopy studies presented earlier relate directly to the formation of ion radicals as CT transients from such weak EDA complexes. By an analogous reasoning, the ground state of strong EDA complexes such as HMB-NO^+ ($K > 10^4 \text{ M}^{-1}$ and ν_{NO} the same as that of free NO) may be described essentially as an EDA complex of the cation radical with NO, i.e. $[\text{HMB}^+, \text{NO}]$. The slope of the correlation in Fig. 15(a) indicates a sharp trend toward the benzene complex in which the ground state can be largely represented by the no-bond structure [with $a \gg b$ in eqn.(56)].

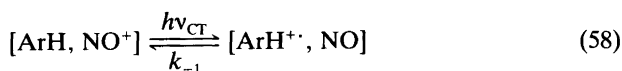
Time-resolved spectral change in the CT excitation of aromatic EDA complexes with NO^+ . The excitation of the charge-transfer band of the aromatic EDA complexes with NO^+ is carried out at $\lambda = 355 \text{ nm}$ using a 30 ns laser pulse. The time-resolved spectrum in Fig. 16 shows the typical bleaching of the CT absorption band (compare Fig. 14 and the appearance of the aromatic cation radical with $\lambda_{\text{max}} \sim$

Table 6. Time-resolved spectroscopy of the CT activation of aromatic EDA complexes with NO^+ .^a

Substituent(s) in benzene	$\lambda(\text{Ar}^+)/\text{nm}$	$k_{-1}/10^6 \text{ s}^{-1}$
None	430	2.7
Cl	470	1.1
Br	540	1.5
I	680	1.4
Me	430	1.2
1,4-Me ₂	440	1.4
1,2,4-Me ₃	455	1.0
1,2,4,5-Me ₄	460	0.66
Me ₅	485	0.30
Me ₆	495	0.15

^aIn dichloromethane solution by CT excitation at 355 nm.

500 nm⁶⁴ [eqn. (58)]. Since no photochemistry occurs upon prolonged irradiation of the CT absorption band (compare



with tropylium complexes described earlier), the subsequent first-order decay of the ArH^+ absorption clearly relates to back electron transfer (k_{-1}). It is significant that the trend in k_{-1} (Table 6) accords with the expected increase in driving force for back electron transfer in proceeding from hexamethylbenzene ($E_i = 7.71 \text{ eV}$) to benzene ($E_i = 9.23 \text{ eV}$). Moreover it is interesting to note that the magnitudes of these rate constants are in line with k'_2 reported in Table 3 for the ion radical pair $[\text{ArH}^+, \text{NO}_2]$ in charge-transfer nitration. Be that as it may be, the time-resolved spectral studies support the notion that ion radical pairs can be held together by CT interactions sufficient to retard their diffusive separation. These preliminary results clearly encourage the further study of the behavior of ion radical pairs that are critical to the understanding of electron transfer, particularly of the ubiquitous inner-sphere processes.

Acknowledgements. I wish to thank my colleagues, especially J. M. Masnovi and S. Sankararaman, for their tireless effort and creative ideas in delineating the transient behavior of ion radical pairs in electron-transfer processes. We thank the National Science Foundation, Texas Advanced Research Program and the Robert A. Welch Foundation for financial support.

References

- Basolo, F. and Pearson, R. G. *Mechanisms of Inorganic Reactions*, Wiley, New York 1967.
- Fukuzumi, S., Wong, C. L. and Kochi, J. K. *J. Am. Chem. Soc.* 102 (1980) 2928.
- Fukuzumi, S. and Kochi, J. K. *Bull. Chem. Soc. Jpn.* 56 (1983) 969.
- (a) Kavarnos, G. J. and Turro, N. J. *Chem. Rev.* 86 (1986) 401; (b) Hoshino, M. and Shizuka, H. In: Fox, M. A. and Chanon, M., Eds., *Photoinduced Electron Transfer*, Part C, Elsevier, Amsterdam 1988, p. 313 ff.
- Jones, G., II, Ref. 4(b), Part A., p. 245 ff; Nagakura, S. In: Lim, E. C., Ed., *Excited States*, Academic Press, New York 1975, Vol. 2; Mataga, N. *Pure Appl. Chem.* 56 (1984) 1255.
- Szwarc, M. *Ions and Ion Pairs in Organic Reactions*, Wiley, New York 1972 and 1974, Vols. 1 and 2.
- Hilinski, E. F., Masnovi, J. M., Kochi, J. K. and Rentzepis, P. M. *J. Am. Chem. Soc.* 106 (1984) 8071.
- Simons, J. D. and Peters, K. S. *Acc. Chem. Res.* 17 (1984) 277; *J. Am. Chem. Soc.* 105 (1983) 4875.
- Fox, M. A. *Adv. Photochem.* 13 (1986) 237.
- (a) Masnovi, J. M., Hilinski, E. F., Rentzepis, P. M. and Kochi, J. K. *J. Am. Chem. Soc.* 108 (1986) 1126; (b) Masnovi, J. M. and Kochi, J. K. *J. Am. Chem. Soc.* 107 (1985) 7880; (c) Sankararaman, S., Haney, W. A. and Kochi, J. K. *J. Am. Chem. Soc.* 109 (1987) 5235, 7824.
- (a) Jones, G., II and Becker, W. G. *Chem. Phys. Lett.* 85 (1982) 271; (b) Jones, G., II and Becker, W. G. *J. Am. Chem. Soc.* 105 (1983) 1276; Peacock, N. J. and Schuster, G. B. *J. Am. Chem. Soc.* 105 (1983) 3632; (c) Masnovi, J. M. and Kochi, J. K. *J. Am. Chem. Soc.* 107 (1985) 6781; (d) Miyashi, T., Kamata, M. and Mukai, T. *J. Am. Chem. Soc.* 109 (1987) 2755, 2780; (e) Takahashi, Y. and Kochi, J. K. *Chem. Ber.* 121 (1988) 253.
- (a) Jones, G., II, Chiang, S. H., Becker, W. G. and Welch, J. A. *J. Phys. Chem.* 86 (1982) 2805; Jones, G. II, Haney, W. A. and Phan, X. T. *J. Am. Chem. Soc.* 110 (1988) 1922; (b) Gould, I. R., Moody, R. and Farid, S. *J. Am. Chem. Soc.* 110 (1988) 7242.
- (a) Benesi, H. G. and Hildebrand, J. H. *J. Am. Chem. Soc.* 71 (1949) 2703; Foster, R. *Molecular Complexes*, Elek Science, London, 1974, Vol. 2, p. 107 ff. (b) Foster, R. *Organic Charge-Transfer Complexes*, Academic Press, New York 1969.
- Mulliken, R. S. *J. Am. Chem. Soc.* 74 (1952) 811; Mulliken, R. S. and Person, W. B. *Molecular Complexes*, Wiley, New York 1969.
- (a) Arnold, D. R. and Maroulis, A. J. *J. Am. Chem. Soc.* 98 (1976) 5931; (b) Reichel, L. W., Griffin, G. W., Muller, A., Das, P. K. and Ege, S. N. *Can. J. Chem.* 62 (1984) 424; Davis, H. F., Das, P. K., Reichel, L. W. and Griffin, G. W. *J. Am. Chem. Soc.* 106 (1984) 6968; Albini, A. and Mella, M. *Tetrahedron* 42 (1986) 6219; (c) Trahanovsky, W. S. and Brixius, D. W. *J. Am. Chem. Soc.* 95 (1973) 6778 [see, however, Baciocchi, E. and Ruzziconi, R. *J. Chem. Soc., Chem. Commun.* (1984) 445 and Camaioni, D. M. and Franz, J. A. *J. Org. Chem.* 49 (1984) 1607]; (d) Maslak, P. and Asel, S. L. *J. Am. Chem. Soc.* 110 (1988) 8260; (e) Hammerich, O. and Parker, V. D. *Adv. Phys. Org. Chem.* 20 (1984) 55.
- (a) Kawai, K., Shirota, Y., Tsubomura, H. and Mikawa, H. *Bull. Chem. Soc. Jpn.* 45 (1972) 77; (b) Kobashi, H., Giyoda, J. and Morita, T. *Bull. Chem. Soc. Jpn.* 50 (1977) 1731; (c) Gschwind, R. and Haselbach, E. *Helv. Chim. Acta* 62 (1979) 941; (d) Kobashi, H., Funabashi, M., Kondo, T., Morita, T., Okada, T. and Mataga, N. *Bull. Chem. Soc. Jpn.* 57 (1984) 3557; (e) Rentzepis, P. M., Steyert, D. W., Roth, H. D. and Abelt, C. J. *J. Phys. Chem.* 89 (1985) 3955.
- (a) Lewis, F. D. *Acc. Chem. Res.* 19 (1986) 401; (b) Refs. 15(c) and 15(d).
- Wasielewski, M. In: Fox, M. A. and Chanon, M., Eds, Ref. 4(b), Part A, p. 161.
- Griller, D. and Ingold, K. U. *Acc. Chem. Res.* 13 (1980) 193.
- (a) Kemula, W., Grabowski, Z. R. and Kalinowski, M. K. *J. Am. Chem. Soc.* 91 (1969) 6863; (b) Penn, J. H., Deng, D. L. and Chai, K. J. *Tetrahedron Lett.* 29 (1988) 3635.
- Kitaigorodski, A. I., Khotyanova, T. L. and Struchkov, Ya. T. *Acta Crystallogr.* 10 (1957) 797.

22. (a) Feldman, M. and Winstein, S. *J. Am. Chem. Soc.* **83** (1961) 3338; (b) Feldman, M. and Graves, B. G. *J. Phys. Chem.* **70** (1966) 955; (c) Dauben, H. J. and Wilson, J. D. *J. Chem. Soc., Chem. Commun.* (1968) 1629.
23. (a) Badger, B. and Brocklehurst, B. *Trans. Faraday Soc.* **65** (1969) 2582; (b) Lau, W. and Kochi, J. K. *J. Org. Chem.* **51** (1986) 1801.
24. Fritz, H. P., Gebauer, H., Friederich, P., Ecker, P., Artes, R. and Schubert, U. *Z. Naturforsch., Teil B* **33** (1978) 498.
25. Takahashi, Y., Sankararaman, S. and Kochi, J. K. *J. Am. Chem. Soc.* **111** (1989) 2954.
26. Masnovi, J. M. and Kochi, J. K. *J. Am. Chem. Soc.* **107** (1985) 6781; see also Ref. 37.
27. Jones, G., II and Becker, W. G. and Peacock, N. J. and Schuster, G. B. In Ref. 11(b).
28. Evans, T. R., Wake, R. W. and Sifain, M. M. *Tetrahedron Lett.* (1973) 701.
29. Ebersson, L. and Nyberg, K. *Adv. Phys. Org. Chem.* **12** (1976) 1; For a recent review, see Yoshida, K. *Electrooxidation in Organic Chemistry*, Wiley, Chichester 1984, p. 156 ff.
30. (a) Mijs, W. J. and de Jonge, C. R. H. I., Eds., *Organic Synthesis by Oxidation with Metal Compounds*, Plenum, New York 1986; Holm, R. H. *Chem. Rev.* **87** (1987) 1401; (b) Sheldon, R. A. and Kochi, J. K. *Metal-Catalyzed Oxidations of Organic Compounds*, Academic, New York 1981.
31. (a) Hofman, K. A. *Ber. Dtsch. Chem. Ges.* **45** (1912) 3329; (b) Hofmann, K. A., Ehrhardt, O. and Schneider, O. *Ber. Dtsch. Chem. Ges.* **46** (1913) 1657; (c) Criegee, R. *Liebigs. Ann. Chem.* **522** (1936) 75; (d) Criegee, R., Marchand, B. and Wannowius, H. *Liebigs. Ann. Chem.* **550** (1942) 99; (e) Schröder, M. *Chem. Rev.* **80** (1980) 187.
32. (a) Nugent, W. A. *J. Org. Chem.* **45** (1980) 4533; (b) Hammond, P. R. and Lake, R. R. *J. Chem. Soc. A* (1971) 3819; (c) Burkhardt, L. A., Hammond, P. R., Knipe, R. H. and Lake, R. R. *J. Chem. Soc. A* (1971) 3789.
33. (a) Cook, J. W. and Schoental, R. *J. Chem. Soc.* (1948) 170; (b) Cook, J. W., Loudon, J. D. and Williamson, W. F. *J. Chem. Soc.* (1950) 911; (c) Criegee, R., Höger, E., Huber, G., Knick, P., Martscheffel, F. and Schellenberger, H. *Justus Liebigs Ann. Chem.* **599** (1956) 81.
34. Cook, J. W. and Schoental, R. *Nature (London)* **161** (1948) 237.
35. Wallis, J. M. and Kochi, J. K. *J. Am. Chem. Soc.* **110** (1988) 8207.
36. Orgel, L. E. and Mulliken, R. S. *J. Am. Chem. Soc.* **79** (1957) 4839.
37. Masnovi, J. M. and Kochi, J. K. Ref. 10(b).
38. Kenner, J. *Nature (London)* **156** (1945) 369.
39. Brown, R. D. *J. Chem. Soc.* (1959) 2224, 2232.
40. (a) Nagakura, S. and Tanaka, J. *J. Chem. Phys.* **22** (1954) 563; (b) Nagakura, S. *Tetrahedron* **19** (Suppl. 2) (1963) 361.
41. Pederson, E. B., Petersen, T. E., Torsell, K. and Lawesson, S.-O. *Tetrahedron* **29** (1973) 579.
42. Perrin, C. L. *J. Am. Chem. Soc.* **99** (1977) 5516.
43. (a) Ebersson, L., Jonsson, L. and Radner, F. *Acta Chem. Scand., Ser. B* **32** (1978) 749; (b) Ebersson, L. and Radner, F. *Acta Chem. Scand., Ser. B* **34** (1980) 739; (c) Ebersson, L. and Radner, F. *Acta Chem. Scand., Ser. B* **39** (1985) 357; (d) Ebersson, L. and Radner, F. *Acta Chem. Scand., Ser. B* **38** (1984); *Acc. Chem. Res.* **20** (1987) 53.
44. Schofield, K. *Aromatic Nitration*, Cambridge University Press, Cambridge, UK 1980.
45. Wheland, G. W. *J. Am. Chem. Soc.* **64** (1942) 900.
46. (a) Hartshorn, S. R. *Chem. Soc. Rev.* **3** (1974) 167; (b) Suzuki, H. *Synthesis* (1977) 217.
47. (a) Parker, W. D. and Ebersson, L. *Tetrahedron Lett.* (1969) 2839, 2843; (b) Schlesener, C. J. and Kochi, J. K. *J. Org. Chem.* **49** (1984) 3142; (c) Kochi, J. K., Tang, R. T. and Bernath, T. *J. Am. Chem. Soc.* **95** (1973) 7114.
48. Melander, L. *Ark. Kemi* **2** (1950) 211; Halvarson, K. and Melander, L. *Ark. Kemi* **11** (1957) 77; Melander, L. *Isotope Effects on Reaction Rates*, Ronald Press, New York 1960.
49. Fukuzumi, S. and J. K. Kochi *J. Am. Chem. Soc.* **103** (1981) 7240.
50. Fischer, A., Fyles, D. L. and Henderson, G. N. *J. Chem. Soc., Chem. Commun.* (1980) 513; Fischer, A., Leonard, D. R. A. and Roderer, R. *Can. J. Chem.* **57** (1979) 5727.
51. Clark, E. P. *J. Am. Chem. Soc.* **53** (1931) 3431.
52. Loudon, J. D. and Ogg, J. *J. Chem. Soc.* (1955) 739.
53. (a) Perrin, C. L. and Skinner, G. A. *J. Am. Chem. Soc.* **93** (1971) 3389; (b) Bunton, C. A., Hughes, E. O., Ingold, C. K., Jacobs, D. J. H., Jones, M. H., Minkoff, G. J. and Reed, R. I. *J. Chem. Soc.* (1950) 2628; (c) Reverdin, F. and Düring, F. *Ber. Dtsch. Chem. Ges.* **32** (1899) 152; (d) Robinson, G. M. *J. Chem. Soc.* **109** (1916) 1078; (e) Barnes, C. E., Feldman, K. S., Johnson, M. W., Lee, H. W. H. and Myhre, P. C. *J. Org. Chem.* **44** (1979) 3925; (f) Barnes, C. E. and Myhre, P. C. *J. Am. Chem. Soc.* **100** (1978) 973.
54. For a theoretical description of aromatic nitrosation, see Minkin, V. I., Minyaev, R. M., Yudilevich, I. A. and Kletskii, M. E. *J. Org. Chem. USSR* **21** (1985) 842.
55. (a) Bandlish, B. K. and Shine, J. J. *J. Org. Chem.* **42** (1977) 561; (b) Ebersson, L. and Radner, F. Ref. 43(d); (c) Musker, W. K., Wolford, T. L. and Roush, P. B. *J. Am. Chem. Soc.* **100** (1978) 6416.
56. (a) Marvel, C. S. and Porter, P. K. *Org. Synth., Coll. Vol. I* (1941) 411; (b) Challis, B. C. and Lawson, A. J. *J. Chem. Soc., Perkin Trans. 2* (1973) 918; (c) For a summary, see March, J. *Advanced Organic Chemistry*, McGraw-Hill, New York 1968, p. 397; Williams, D. L. H., *Nitrosation*, Cambridge University Press, Cambridge, UK 1988.
57. (a) Hunziker, E., Penton, J. R. and Zollinger, H. *Helv. Chim. Acta* **54** (1971) 2043; (b) Brownstein, S., Gabe, E., Lee, F. and Tan, L. *J. Chem. Soc., Chem. Commun.* (1984) 1566.
58. Brownstein, S., Gabe, E., Lee, F. and Piotrowski, A. *Can. J. Chem.* **64** (1986) 1661.
59. Kim, E. K. *Unpublished results*.
60. Kim, E. K. and Kochi, J. K. *J. Org. Chem.* **54** (1989) 1692.
61. Kamar, E. and Neilands, O. *Russ. Chem. Rev.* **55** (1986) 334.
62. (a) Kamar, V. E., Valtere, S. P. and Neiland, O. Ya. *Theor. Exp. Chem. (USSR)* **14** (1978) 288; (b) Kamar, V. E., Gudele, I. Ya. and Neiland, O. Ya. *Theor. Exp. Chem. (USSR)* **16** (1980) 321; (c) Chappell, J. S., Block, A. N., Bryden, W. A., Maxfield, M., Poehler, T. O. and Cowan, D. O. *J. Am. Chem. Soc.* **103** (1981) 2442.
63. Hanna, M. W. In: Foster, R., Ed., *Molecular Complexes*, Elek Science, London 1973, p. 1 ff.
64. Sankararaman, S. *Unpublished results*.

Received August 8, 1989.